showed that the xenobiotic response of CYP2E1 up-regulation mediated by AhR for benzene hematotoxicity was metabolized specifically in the BM (Hirabayashi et al., 2005a). In this article, the detailed changes in blood parameters during the benzene exposure duration and their recovery three days after the cessation of exposure are shown.

2. Materials and methods

2.1. Animals

The establishment of homozygous AhR-KO ($AhR^{-/-}$) mice originating from the 129/SvJ strain has been described elsewhere (Mimura et al., 1997; Yoon et al., 2002). The crossing of heterozygous AhR-KO ($AhR^{+/-}$) males with $AhR^{+/-}$ females generated wild-type ($AhR^{+/+}$), $AhR^{+/-}$, and $AhR^{-/-}$mice. The neonates were genotyped by PCR screening of DNA from the tail. Male AhR-KO ($AhR^{-/-}$) mice and their Wt littermates (12 weeks old) were used in the study as donors. Eight-week-old C57BL/6 male mice from Japan SLC (Shizuoka, Japan) were used as recipients for the repopulation assay and the assay of colony-forming unit in the spleen (CFU-S). All the mice were housed under specific pathogen-free conditions at 24 ± 1 °C and 55 ± 10% relative humidity, under a 12-h light dark cycle. Autoclaved tap water and food pellets were provided *ad libitum*.

2.2. Benzene and benzene exposure

Benzene, CAS. No. 71-43-2, MW 78.11, was purchased from Wako Fine Chemical Company (Osaka, Japan). Experimental mice were intragastrically (*i.g.*) administered with freshly prepared corn oil solutions of benzene (150 mg/kg body weight) once daily for 5 days/week for 2 weeks). The dose used in this study was 150 mg/kg body weight which corresponds to the daily dose for leukemic induction, that is, 300 ppm for 6 h/day (Cronkite et al., 1984; Li et al., 2006). Both doses administered for 5 days/week for 26 weeks induce hematopoietic malignancies at the highest frequency. The aim of this study using this dose is to examine the corresponding toxicity of benzene for inducing hematopoietic malignancies. Note, this dose is over 100-fold higher than the occupational tolerable exposure dose.

2.3. Blood and BM parameters

Peripheral blood was collected from the orbital sinus. Peripheral blood leukocyte (WBC), red blood cell (RBC) and platelet (PLT) counts were determined using a blood cell counter (Sysmex K-4500, Sysmex Co., Kobe, Japan). BM cellularity was evaluated by harvesting BM cells from the femurs of each mouse (Yoon et al., 2001). The animals were sacrificed on days 5, 12, and 15 to evaluate recovery. Then, a 27-gauge needle was inserted into the femoral bone cavity through the proximal and distal edges of the bone shafts, and BM cells were flushed out under pressure by injecting 2 ml of α-MEM. A single-cell suspension was obtained by gently triturating the BM cells through the 27-gauge needle, and cells were counted using the Sysmex K-4500.

2.4. Irradiation

Recipient mice were exposed to a lethal radiation of 800.1 cGy, at a dose rate of 124 cGy/min, using a ^{137}Cs-gamma irradiator (Gammacell 40 Exactor, MDS Nordin Inc., Canada) with a 0.5 mm aluminum–copper filter.

2.5. CFU-S assay

The Till and McCulloch method (Till and McCulloch, 1961) was used for determining the number of colony-forming units in the spleen (CFU-S). Aliquots of BM cell suspensions were used for evaluating the number of CFU-S. The number of BM cells was adjusted to that appropriate for producing non-confluent spleen colonies, and the cells were then transplanted into lethally irradiated mice by injection through the tail vein. Spleens were harvested nine and 13 days after the injection, and fixed in Bouin's solution. Macroscopic spleen colonies were counted under an inverted microscope at a magnification of 5.6×.

2.6. Assays for CFU-GM and CFU-E

Colony formation *in vitro* was assayed in a semisolid methylcellulose culture (Yoon et al., 2001; Hirabayashi et al., 2002a). Briefly, 8×10^4 BM cells suspended in 100 μl of a medium were added to 3.9 ml of a culture medium containing 0.8% methylcellulose, 30% fetal calf serum, 1% bovine serum albumin, 10^{-4} M 2-mercaptoethanol, with 10 ng/ml murine granulocyte-macrophage colony-stimulating factor (GM-CSF) for CFU-GM assay or 1 ng/ml murine interleukin-3 and 2 U/ml erythropoietin for erythroid CFU (CFU-E) assay. One-milliliter aliquots containing 2×10^4 BM cells were plated in triplicate in a 35-mm tissue culture plate, and incubated for six days in a completely humidified incubator at 37 °C with 5% CO_2 in air. Under an inverted microscope, CFU-GM after a six-day culture was counted at a magnification of 40× and CFU-E after a three-day culture at 100×.

2.7. BM repopulation assay

BM repopulation assay (Hirabayashi et al., 1992) was performed similarly to the assay of CFU-S, except that 1×10^6 BM cells were injected into lethally irradiated mice. One month after the transfusion of BM cells, the repopulated mice exposed to benzene.

3. Results and discussion

As previously reported, the AhR-KO mice showed a significantly higher WBC counts than the Wt mice (Fig. 1a). This was also consistent with the high number of myeloid progenitor cells, that is, CFU-S-9 and CFU-S-13, observed in the AhR-KO mice (Fig. 1b). Thus, steady-state hemopoiesis in the Wt mice, on the other hand, is presumed to be suppressed by AhR signaling because of the possible presence of a physiological ligand, which is not readily observed in the AhR-KO mice. In contrast, the numbers of mature progenitor cells in the BM, that is, CFU-E and CFU-GM, decreased (Fig. 1c). This is assumed to be due to a homeostatic negative regulation for the above-mentioned increase in the number of immature myeloid progenitor cells, although direct evidence for a possible feedback was not obtained. These lines of experimental evidences from the AhR-KO mice suggest that the numbers of mature progenitor cells, CFU-E, and CFU-GM in the Wt mice increase.

The assumption that immature progenitor cells in the Wt mice are suppressed by AhR signaling, however, is inconsistent with some reports that certain cell lines showed an enhanced proliferation in the presence of AhR signaling (Ma and Whitlock, 1996; Shimba et al., 2002). In the case of the A549 cell line, cells proliferated by AhR overexpression with the presence of ligands (Shimba et al., 2002). In the case of Hepa 1c1c7, the cell line, cell proliferation was suppressed with deceleration of cell cycling, when antisense AhR was introduced to the cell line (Ma and Whitlock, 1996). Our interpretation of these inconsistent reports is based

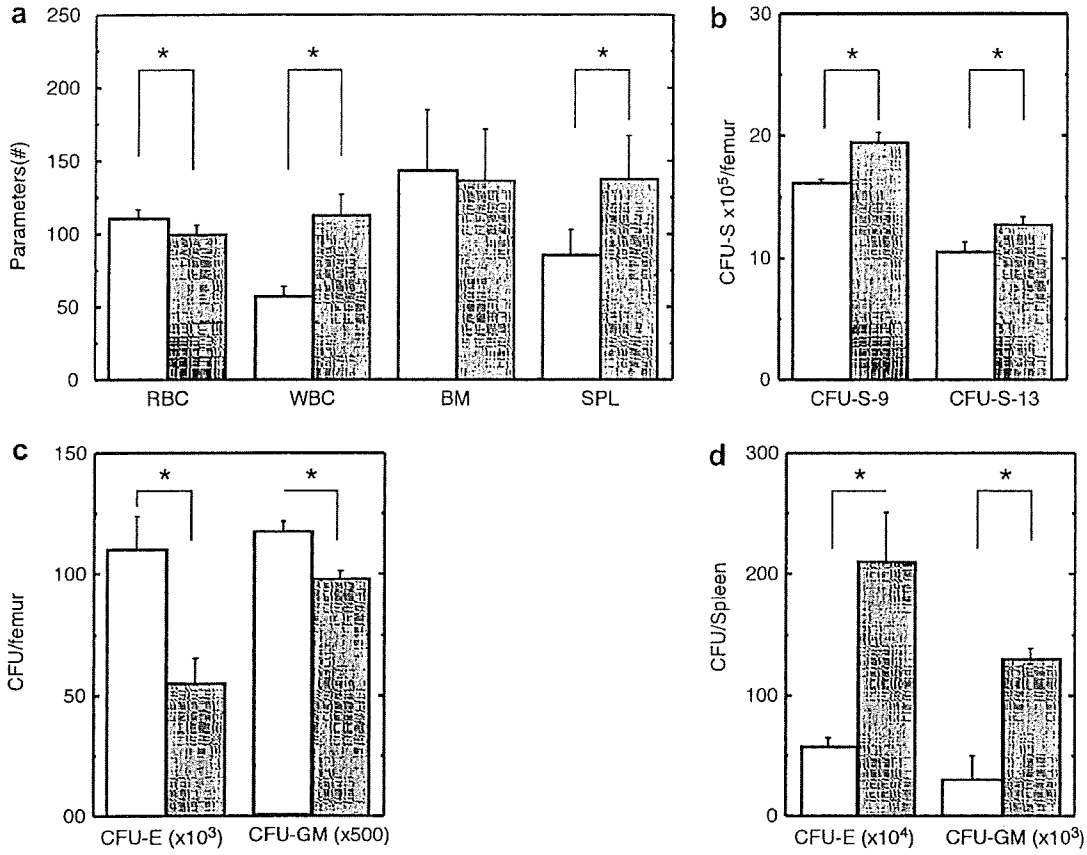

Fig. 1. Comparison of various blood parameters between Wt mice (open columns) and AhR-KO mice (shaded columns). (a) Peripheral blood, bone marrow (BM) and spleen weight. #: vertical axis "Parameters" indicate the counts of peripheral red blood cells (RBCs, $\times 10^8$/ml) and white blood cells (WBCs, $\times 10^6$/ml), BM cellularity ($\times 10^5$/femur), and weight of the spleen (SPL, mg). (b) Number of colony-forming units in spleen (CFU-S, $\times 10^5$/femur) observed on days 9 (CFU-S-9) and 13 (CFU-S-13). (c) Numbers of *in vitro* granulocyte- macrophage CFUs (CFU-GM, ×500/femur) and erythroid CFU (CFU-E, $\times 10^3$/ femur) in femoral BM. (d) Numbers of CFU-GM ($\times 10^3$/spleen) and CFU-E ($\times 10^4$/spleen) in the spleen. * : Significant difference between Wt and AhR-KO mice determined by *t*-test at $p < 0.05$.

on *in vitro* characteristics, that is, the A549 cell line was reported to show an altered p27 expression, and Hepa 1c1c7 cells were supposed to maintain their its survival by AhR signaling. Moreover, a contradictory report was also found in which artificial AhR signaling suppression induced cellular proliferation (Fong et al., 2005). The above-mentioned evidence suggests that the receptor function in the presence or absence of a ligand may differ; therefore, it is of interest to determine whether signaling from AhR in Wt mice that suppressed cell proliferation might be altered by ligand signals.

Taking together the above lines of evidence, the function of AhR signaling is presumed to be expressed solely in immature progenitor cells, which suppresses their proliferation, maintains their quiescence, and thereby, conserves the characteristic features of stem cells, that is, stemness.

Interestingly, in response to such an AhR-null effect, the AhR-KO mice contrarily showed extensive hemopoiesis in the spleen (Fig. 1d), which resulted in a significant increase in spleen weight (Fig. 1a; most right) (Hirabayashi et al., 2003, 2005a).

Because of the above-mentioned difference in BM function between the AhR-KO mice and the Wt mice, in this study, benzene-induced hematotoxicity was evaluated in the Wt mice after subjecting them to a lethal dose of whole-body irradiation followed by repopulation with BM cells that lack AhR. Six weeks after the repopulation, the steady-state hematopoietic parameters for repopulated mice were obtained and are shown in Fig. 2a and b. The results were essentially the same between the mice repopulated with Wt BM cells (open columns) and those repopulated with AhR-KO BM cells (shaded columns) except that there is no anemic tendency, leukocytotic change, nor evidence of splenomegaly in Wt mice as compared with the AhR-KO mice as shown in Fig. 1.

Fig. 3a and b shows the percentages of RBCs (a) and WBCs (b) with respect to the control in the peripheral blood after the repopulation with BM cells. In the Wt mice repopulated with Wt BM cells and those with AhR-KO BM cells (open and closed symbols, respectively), benzene exposure induced a slight but statistically significant decrease in RBC count compared with the sham-exposure except on day 5 in the Wt groups (100% with standard deviation of the mean indicated by horizontal lines: Fig. 3a). The dose used in the present study was sufficiently high, and the decrease in RBC count was readily observed within 2 weeks of exposure.

The decreases in WBC count shown in Fig. 3b are more significant than those in RBC count throughout the exposure period except on day 5 in the AhR-KO group (the data were significantly different between Wt mice ($50.8 \pm 11.2\%$) and AhR-KO mice ($70.6 \pm 17.6\%$; $p = 0.024$)). In contrast to the previous observation (data not shown), mice repopulated with AhR-KO BM cells showed no significant difference in decrease of RBCs or WBCs. This difference in the observation of AhR-KO BM cells between the previous experiment and this study may be due to the difference in the route of benzene exposure, that is, intraperitoneal (*i.p.*) and intragastric (*i.g.*), respectively. Despite BM repopulation with AhR-KO BM cells, benzene exposure by the *i.g.* route in this study may have induced portal hepatic drug metabolism at a much greater extent than that by the *i.p.* exposure route. There was no significant differ-

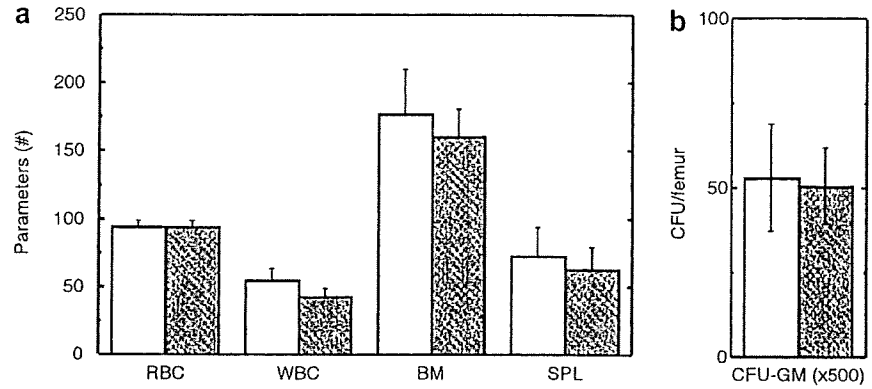

Fig. 2. Comparison of various blood parameters between mice repopulated with Wt BM (open columns) and AhR-KO BM (shaded columns) cells. (a) Peripheral blood, BM and spleen weight. #: vertical axis "Parameters" indicate the counts of peripheral RBCs ($\times 10^8$/ml) and WBCs ($\times 10^6$/ml), BM cellularity ($\times 10^5$/femur), and weight of the spleen (SPL, mg). (b) Numbers of CFU-GM (5×10^2/femur) per femur.

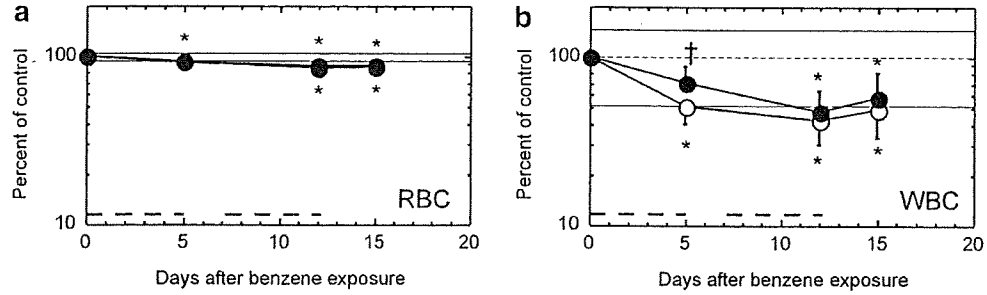

Fig. 3. Changes in percentage numbers of RBC (a) and WBC (b) of mice repopulated with Wt BM (open symbols) and AhR-KO BM (closed symbols) cells during and after benzene exposure, with respect to each sham-exposure group. Vertical bars indicate the standard deviation of the mean. Horizontal dashed line indicates the mean (100%) and the solid lines indicate the standard deviation of the mean (100%) from the sham-exposure control Wt group. The dashed line at the bottom indicates benzene exposure duration. *: Significant difference between sham-exposure group and benzene-exposed group determined by *t*-test at $p < 0.05$. †: Significant difference between Wt mice and AhR-KO mice.

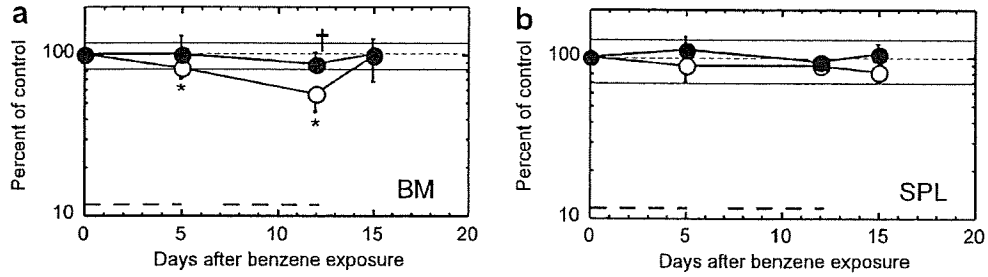

Fig. 4. Changes in percentage number of BM cells (a) and weight of spleen (b) of mice repopulated with Wt BM (open symbols) and AhR-KO BM (closed symbols) cells during and after benzene exposure, with respect to each sham-exposure group. Vertical bars indicate the standard deviation of the mean. Horizontal dashed line indicates the mean (100%) and the solid lines indicate the standard deviation of the mean (100%) from the sham control Wt group. The dashed line at the bottom indicates benzene exposure duration. *: Significant difference between sham-exposure group and benzene-exposed group determined by *t*-test at $p < 0.05$. †: Significant difference between Wt mice and AhR-KO mice.

ence in data between the Wt mice and AhR-KO mice except on day 5 in the number of WBCs.

As shown in Fig. 4a, the decrease in the number of BM cells after benzene exposure is significant in the mice repopulated with Wt BM cells specifically on days 5 and 12 (82.2 ± 12.0%, $p = 0.035$ and 65.4 ± 20.3%, $p = 0.007$, respectively; number of cells obtained on day 12 was also significantly different between the Wt mice and the AhR-KO mice (86.7 ± 14.9%; $p = 0.013$)), which returned to the normal range by day 15, that is, three days after cessation of benzene treatment. In contrast to the peripheral blood parameters (Fig. 3a and b), the number of BM cells in the mice repopulated with AhR-KO BM cells did not show any decrease, but the mice showed a clear nullification of benzene-induced decrease in the number of BM cells (86.7 ± 14.9%; $p = 0.057$). Concerning the weight of the spleen, there are no significant differences among the groups regardless of the duration of benzene treatment and AhR expression (Fig. 4b).

In Fig. 5, the number of CFU-GM in the BM of mice repopulated with Wt BM cells much more significantly decreased on day 12 (open symbols, 37.8 ± 14.2%, $p = 0.019$; the number was also significantly different between Wt mice and AhR-KO mice (82.0 ± 7.0%; $p = 0.0008$)), which quickly returned to the normal range by day

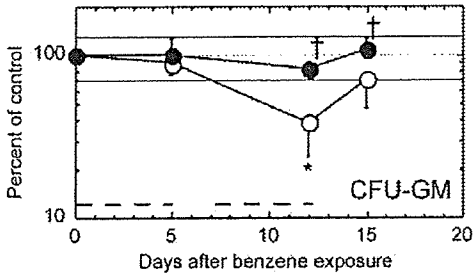

Fig. 5. Changes in percentage number of CFU-GM of mice repopulated with Wt BM (open symbols) and AhR-KO BM (closed symbols) cells during and after benzene exposure, with respect to each sham-exposure group. Vertical bars indicate the standard deviation of the mean. Horizontal dashed line indicates the mean (100%) and the solid lines indicate the standard deviation of the mean (100%) from the sham-exposure control Wt group. The dashed line at the bottom indicates benzene exposure duration. *: Significant difference between sham-exposure group and benzene-exposed group determined by *t*-test at $p < 0.05$. †: Significant difference between Wt mice and AhR-KO mice.

15, three days after cessation of benzene treatment. In this figure, interestingly, the benzene-induced decrease in the number of CFU-GM in the BM of mice repopulated with the AhR-KO BM cells (closed symbols) is clearly nullified for the Wt BM cells (open symbols), and the number stays within the range found for the sham-exposure. The reason for this much prominent decrease observed in the number of CFU-GM in the case of benzene exposure may be due, in part, to the expression of AhR, whose level is significantly high in primitive hematopoietic progenitor cells (Hirabayashi et al., 2002b, 2005b), the KO of which nullified the decrease in the number of CFU-GM much more significantly than the decrease in peripheral blood parameters.

4. Conclusions

Mice that had been lethally irradiated and repopulated with BM cells from AhR-KO mice essentially did not show any benzene-induced hematotoxicity. The present study elucidated the following: first, benzene-induced decrease in BM cellularity was clearly nullified by BM cells in mice that had been repopulated with AhR-KO BM cells. Second, we observed some differences in toxicologic phenotypes depending on the exposure route, that is, intraperitoneal, used in the previous study, or intragastric, in this study; that is, the former route induced attenuation of significant decreases in RBC number, spleen weight, and CFU-GM number, whereas the latter route induced attenuation of decrease in BM cellularity and CFU-GM number as compared with the Wt mice, respectively. Third, the marked decrease in the number of CFU-GM following benzene treatment and its nullification by repopulation with AhR-KO BM cells are the essential key discoveries of this study that may be related to the expression of AhR in primitive hematopoietic progenitor cells. Together with our previous observation and the report on the expression of CYP2E1 (Yoon et al., 2003; Ivanova et al., 2002), findings in this study may be related to the expression of CYP2E1 in BM cells.

Acknowledgments

This work was supported in part by a Grant-in-Aid for Scientific Research C, 15510064 and also by the MHLW-Research Fund (H16-Chemistry 003), National Institute of Health Sciences.

We thank Ms. E. Tachihara, Ms. Y. Usami, Ms. Y. Shinzawa, and Ms. M. Uchiyama for excellent technical assistance, and Ms. N. Kikuchi, M. Yoshizawa, and Ms. M. Hojo for secretarial assistance.

References

Cronkite, E.P., Bullis, J., Inoue, T., Drew, R.T., 1984. Benzene inhalation produces leukemia in mice. Toxicol. Appl. Pharmacol. 75, 358–361.

Fong, C.J., Burgoon, L.D., Zacharewski, T.R., 2005. Comparative microarray analysis of basal gene expression in mouse Hepa-1c1c7 wild-type and mutant cell lines. Toxicol. Sci. 86, 342–353.

Garrett, R.W., Gasiewicz, T.A., 2005. The arylhydrocaron receptor (AhR) is a regulator of hematopoietic stem and progenitor cell growth. Meeting abstract, Molecular Regulation of Stem Cell, Keystone symosia, p. 61.

Hirabayashi, Y., Inoue, T., 2005b. Chapter 24. Toxicogenomics applied to hematotoxicology. In: Borlak, J. (Ed.), Handbook of Toxicogenomics. Wiley-VCH, Verlag GmbH, Weinheim, pp. 583–608.

Hirabayashi, Y., Inoue, T., Suda, Y., Aizawa, S., Ikawa, Y., Kanisawa, M., 1992. Hemopoietic neoplasms in lethally irradiated mice repopulated with bone marrow cells carrying the human c-myc oncogene: a repopulation assay. Exp. Hematol. 20, 167–172.

Hirabayashi, Y., Matsuda, M., Aizawa, S., Kodama, Y., Kanno, J., Inoue, T., 2002a. Serial transplantation of p53-deficient hemopoietic progenitor cells to assess their infinite growth potential. Exp. Biol. Med. (Maywood) 22, 474–479.

Hirabayashi, Y., Miyajima, A., Yokota, T., Arai, K.-I., Li, G.X., Yoon, B.I., Kaneko, T., Kanno, J., Inoue, T., 2002b. Effect of 2,3,7,8-tetrachlorodibenzo-*p*-dioxin (TCDD) on B cell differentiation in mouse pre-B colonization model regulated by artificially introduced human IL-3 receptors. Organohalogen Comp. 55, 359–362.

Hirabayashi, Y., Li, G., Yoon, B.I., Fujii-Kuriyama, Y., Kaneko, T., Kanno, J., Inoue, T., 2003. AhR suppresses hemopoiesis during steady state but accelerates cell cycle as an early response: a study of AhR-knockout mice. Organohalogen Comp. 64, 270–273.

Hirabayashi, Y., Yoon, B.I., Li, G., Fujii-Kuriyama, Y., Kaneko, T., Kanno, J., Inoue, T., 2005a. Benzene-induced hematopoietic toxicity transmitted by AhR in the wild-type mouse was negated by repopulation of AhR deficient bone marrow cells. Organohalogen Comp. 67, 2280–2283.

Ivanova, N.B., Dimos, J.T., Schaniel, C., Hackney, J.A., Moore, K.A., Lemischka, I.R., 2002. A stem cell molecular signature. Science 298, 601–604.

Li, G.X., Hirabayashi, Y., Yoon, B.I., Kawasaki, Y., Tsuboi, I., Kodama, Y., Kurokawa, Y., Yodoi, J., Kanno, J., Inoue, T., 2006. Thioredoxin overexpression in mice, model of attenuation of oxidative stress, prevents benzene-induced hemato-lymphoid toxicity and thymic lymphoma. Exp. Hematol. 34, 1687–1697.

Ma, Q., Whitlock Jr., J.P., 1996. The aromatic hydrocarbon receptor modulates the Hepa 1c1c7 cell cycle and differentiated state independently of dioxin. Mol. Cell Biol. 16, 2144–2150.

Mimura, J., Yamashita, K., Nakamura, K., Morita, M., Takagi, T.N., Nakao, K., Ema, M., Sogawa, K., Yasuda, M., Katsuki, M., Fujii-Kuriyama, Y., 1997. Loss of teratogenic response to 2,3,7,8-tetrachlorodibenzo-*p*-dioxin (TCDD) in mice lacking the Ah (dioxin) receptor. Genes Cells 2, 645–654.

Shimba, S., Komiyama, K., Moro, I., Tezuka, M., 2002. Overexpression of the aryl hydrocarbon receptor (AhR) accelerates the cell proliferation of A549 cells. J. Biochem. (Tokyo) 132, 795–802.

Till, J.E., McCulloch, E.A., 1961. A direct measurement of the radiation sensitivity of normal mouse bone marrow cells. Radiat. Res. 14, 213–222.

Yoon, B.I., Hirabayashi, Y., Kawasaki, Y., Kodama, Y., Kaneko, T., Kim, D.Y., Inoue, T., 2001. Mechanism of action of benzene toxicity: cell cycle suppression in hemopoietic progenitor cells (CFU-GM). Exp. Hematol. 29, 278–285.

Yoon, B.I., Hirabayashi, Y., Kawasaki, Y., Kodama, Y., Kaneko, T., Kanno, J., Kim, D.Y., Fujii-Kuriyama, Y., Inoue, T., 2002. Aryl hydrocarbon receptor mediates benzene-induced hematotoxicity. Toxicol. Sci. 70, 150–156.

Yoon, B.I., Li, G.X., Kitada, K., Kawasaki, Y., Igarashi, K., Kodama, Y., Inoue, T., Kobayashi, K., Kanno, J., Kim, D.Y., Inoue, T., Hirabayashi, Y., 2003. Mechanisms of benzene-induced hematotoxicity and leukemogenicity: cDNA microarray analyses using mouse bone marrow tissue. Environ. Health Perspect. 111, 1411–1420.

Original Article

Sexual Development

Sex Dev 2008;2:1–11
DOI: 10.1159/000117714

Received: May 18, 2007
Accepted: January 2, 2008

Disruption of Aryl Hydrocarbon Receptor (AhR) Induces Regression of the Seminal Vesicle in Aged Male Mice

T. Baba[a] Y. Shima[a] A. Owaki[a] J. Mimura[b] M. Oshima[b] Y. Fujii-Kuriyama[b, c] K.-i. Morohashi[a, c]

[a]Division of Sex Differentiation, National Institute for Basic Biology, National Institutes of Natural Sciences, Higashiyama, Myodaiji-cho, Okazaki, Aichi, [b]TARA Center, University of Tsukuba, Tennoudai, Tsukuba, Ibaraki, [c]Solution Oriented Research for Science and Technology, Japan Science and Technology Agency, Honcho, Kawaguchi, Saitama, Japan

Key Words

AhR(–/–)males · Aryl hydrocarbon receptor (AhR) · 3βHsd · Mice · Seminal vesicle regression · Testes · Testosterone

Abstract

The aryl hydrocarbon receptor (AhR) is a ligand-activated transcription factor that mediates diverse dioxin toxicities. Despite mediating the adverse effects, the *AhR* gene is conserved among animal species, suggesting important physiological functions for AhR. In fact, a recent study revealed that AhR has an intrinsic function in female reproduction, though its role in male reproduction is largely unknown. In this study, we show age-dependent regression of the seminal vesicles, probably together with the coagulating gland, in *AhR*(–/–) male mice. Knockout mice had abnormal vaginal plugs, low sperm counts in the epididymis, and low fertility. Moreover, serum testosterone concentrations and expression of steroidogenic 3βhydroxysteroiddehydrogenase (3βHsd) and steroidogenic acute regulatory protein (StAR) in testicular Leydig cells were decreased in *AhR*(–/–) males. Taken together, our results suggest that impaired testosterone synthesis in aged mice induces regression of seminal vesicles and the coagulating glands. Such tissue disappearance likely resulted in abnormal vaginal plug formation, and eventually in low fertility. Together with previous findings demonstrating AhR function in female reproduction, AhR has essential functions in animal reproduction in both sexes.

The aryl hydrocarbon receptor (AhR) is a ligand-activated transcription factor belonging to the basic helix-loop-helix (bHLH)-PAS (Per-AhR/Arnt-Sim) super-gene family [Burbach et al., 1992; Ema et al., 1992]. Since AhR can bind with 2,3,7,8-tetrachlorodibenzo-*p*-dioxin (TCDD, dioxin) [Poland et al., 1976; Ema et al., 1992], the molecular properties of AhR as a transcription factor have been extensively studied, especially focusing on the transactivation of a series of drug-metabolizing enzyme genes including *Cyp1a1* [Fujisawa-Sehara et al., 1987; Hankinson, 1995; Mimura and Fujii-Kuriyama, 2003]. In addition to these in vitro studies, in vivo gene disruption studies have revealed that AhR mediates a variety of toxicological effects of dioxin including teratogenesis, immunosuppression, tumor promotion, and estrogenic function [Poland and Knutson, 1982; Gibbons, 1993; Mimura et al., 1997; Brown et al., 1998; Shimizu et al., 2000]. Despite promoting these multiple adverse effects, the *AhR* gene is conserved across a variety of animal species from invertebrates to vertebrates [Hahn, 2002], suggesting that in addition to mediating the response to xenobiotics, there are intrinsic functions for AhR in physiological processes.

Recently, the intrinsic functions of AhR have been investigated with regards to animal reproduction and liver vasculogenesis. Indeed, recent studies in *AhR*(–/–) mice demonstrated that AhR is involved in female reproduction by regulating estradiol synthesizing *Cyp19* (P450

KARGER

Fax +41 61 306 12 34
E-Mail karger@karger.ch
www.karger.com

1661–5425/08/0021–0001$24.50/0

Accessible online at:
www.karger.com/sxd

Ken-ichirou Morohashi
Division of Sex Differentiation, National Institute for Basic Biology
National Institutes of Natural Sciences, 5-1 Higashiyama, Myodaiji-cho
Okazaki, Aichi 444-8787, Japan
Tel. +81 564 59 5865, Fax +81 564 59 5866, E-Mail moro@nibb.ac.jp

aromatase) gene expression [Baba et al., 2005] and vessel remodeling in the liver [Lahvis et al., 2005]. Based on the essential functions of estradiol in the female reproductive process such as folliculogenesis, ovulation, and implantation [Fisher et al., 1998; Dupont et al., 2000; Curtis Hewitt et al., 2002], it was concluded that AhR plays an indispensable function in female reproduction. Moreover, in the case of male reproduction, dioxins were reported to reduce epididymal and ejaculated sperm number [Gray et al., 1995; Sommer et al., 1996], implicating that AhR is involved in the male reproductive process. However, there is no direct evidence for the involvement of AhR in this process.

The accessory internal reproductive systems, derived from the Wolffian duct for males and from the Mullerian duct for females, are clearly different between the two sexes. The male internal reproductive system consists of multiple tissues such as the epididymis, the deferens duct, the seminal vesicle, the coagulating gland, and the ejaculatory duct. Developmentally, all these tissues are known to be regulated by androgen signaling [Cunha, 1972; Cooke et al., 1991]. The mature seminal vesicle consists of numerous outpouchings of alveolar glands that empty into the ejaculatory duct. Although semen mostly contains materials secreted from the seminal vesicle, a definite functional relationship linking the seminal vesicle to male fertility has yet to be elucidated. The coagulating gland secretes a substance that, when mixed with the secretions from the seminal vesicle, forms a vaginal plug, and it has been thought that the vaginal plug is required for efficient pregnancy after insemination.

In this study, we define a novel phenotype of *AhR*(–/–) male mice. Interestingly, the seminal vesicle and probably the coagulating gland regressed in an age-dependent manner in the *AhR*(–/–) mouse, and such regression is possibly due to a low level of serum testosterone. These abnormalities possibly produce an abnormal vaginal plug and decrease the fertility of the male mice. This finding together with the previous finding in female reproductive processes [Baba et al., 2005] strongly suggests that AhR greatly influences animal reproduction regardless of the sex.

Materials and Methods

Mice

Targeted disruption of the *AhR* gene was performed as described previously [Mimura et al., 1997]. AhR knockout mice used in this study were backcrossed to C57BL/6J for more than eight generations in order to avoid experimental variation due to genetic background.

Antibodies

A full-length cDNA for mouse 3βHsd1 was kindly provided by Dr. A. Payne (Stanford University). A prokaryotic expression vector for 3βHsd was constructed by insertion of the 3βHsd cDNA into pET-28a (Novagen, San Diego, CA). Preparation of recombinant 3βHsd protein and immunization of rabbits were described previously [Morohashi et al., 1993]. Rabbit antibodies for AhR and Cyp19 were generously provided by Dr. R. Pollenz (University of South Florida) and Dr. N. Harada (Fujita Health University), respectively. Rabbit antibody for androgen receptor (AR) was purchased from Santa Cruz Biotechnology (Santa Cruz, CA).

Fertility Assessment

Thirty *AhR*(+/+) wild-type males, three *AhR*(–/–) males harboring the seminal vesicle, and nine *AhR*(–/–) males lacking the seminal vesicle were mated with *AhR*(+/+) females for 5 days. Twelve days after mating, the female mice were sacrificed to determine whether they became pregnant or not. The presence of the seminal vesicle in each *AhR*(–/–) male was determined both one week prior to the mating and just after the mating was completed. Statistical analysis was performed by Fisher's exact test. All protocols for animal experimentation were approved by the Institutional Animal Care and Use Committee of the National Institute for Basic Biology.

Immunohistochemistry and Western Blot

To detect AhR and AR, cryosections (10 μm) were prepared from the seminal vesicle treated overnight with 4% paraformaldehyde at 4°C. After washing with phosphate-buffered saline (PBS), the sections were boiled for 10 min in 10 mM sodium citrate (pH 7.0) to unmask antigen epitopes, followed by treatment with 0.3% H_2O_2 in methanol for 20 min at –20°C. The sections were incubated overnight at 4°C with anti-AhR or anti-AR antibody, washed with PBS, and then incubated with biotinylated donkey anti-rabbit IgG for 3 h at room temperature. After washing, the sections were incubated with horseradish peroxidase-conjugated streptavidin, and then visualized with diaminobenzidine at room temperature. To detect AhR and 3βHsd in the testes, 5 μm paraffin sections were prepared from 4% paraformaldehyde-fixed testes. After deparaffinization, antigen epitopes were unmasked by treatment with 20 μg/ml proteinase K (Sigma Chemical Co., St. Louis, MO) for 10 min at room temperature for AhR or unmasked by boiling for 10 min in 10 mM sodium citrate (pH 7.0) for 3βHsd, followed by treatment with 0.3% H_2O_2 in methanol for 20 min at –20°C. The sections were incubated overnight at 4°C with the anti-AhR or anti-3βHsd antibody, washed with PBS, and then incubated with biotinylated donkey anti-rabbit IgG or Cy-3 conjugated goat anti-rabbit IgG for 3 h at room temperature. After washing, sections immunoreacted with biotinylated antibodies were incubated with horseradish peroxidase-conjugated streptavidin, and then visualized with diaminobenzidine. The sections immunoreacted with Cy-3-conjugated antibody were counterstained with DAPI (2-(4-amidinophenyl)-1H-indole-6-carboxamidine), and then 3βHsd-positive cells were counted under fluorescence microscope.

To prepare whole tissue lysate for Western blot analysis, tissues were lysed with a cell-lysis buffer containing 50 mM Tris-HCl (pH 8.0), 50 mM NaCl, 1 mM EDTA (pH 8.0), and 1% SDS. Next, 10 μg of whole tissue lysates were subjected to SDS-PAGE followed by Western blot analyses using the antibodies for AhR, AR, Cyp19, Ad4BP/SF-1 and 3βHsd, as described previously [Morohashi et al., 1994].

Determination of Serum Testosterone Concentrations

Four *AhR*(+/+) and three *AhR*(−/−) 24-week-old and eight *AhR*(+/+) and ten *AhR*(−/−) 52-week-old male mice were anesthetized with diethyl ether for collection of blood samples. After isolating the serum fraction, serum testosterone concentration was determined by enzyme immunoassay (Cayman Chemical Company, Ann Arbor, MI) according to the protocol provided by the manufacturer.

Sperm Count

Count of epididymal sperm number was performed as reported previously [Bell et al., 2007]. Briefly, the cauda epididymis was dissected and pierced three times with a scalpel blade. Then, the tissue was incubated in 5 ml of PBS containing 0.57% (w/v) BSA at 37°C for 90 min. After incubation, the number of sperms was counted under a microscope.

Leydig Cell Count

Serial sections of the testes prepared from eight *AhR*(+/+) and ten *AhR*(−/−) 52-week-old mice were stained with anti-3βHsd antibody and DAPI. The number of 3βHsd-positive Leydig cells was counted under a fluorescence microscope in 32 sections (4 sections for each animal) of *AhR*(+/+) and 40 sections of *AhR*(−/−).

Quantitative RT-PCR

Quantitative RT-PCR was performed with a 7500 real-time PCR system (Applied Biosystems, Foster City, CA) using Power SYBR Green PCR master mix (Applied Biosystems). The thermal-cycling condition was 50 cycles of 15 s at 95°C and 1 min at 60°C. Primer pairs used for quantitative RT-PCR were as follows: 3βHsd (fwd), 5′-CAG ACC ATC CTA GAT GTC-3′; 3βHsd (rev), 5′-ACT GCC TTC TC GCC ATC-3′; StAR (fwd), 5′-CCG GAG CAG AGT GGT GTC A-3′; StAR (rev), 5′-GCC AGT GGA TGA AGC ACC AT-3′; Insl3 (fwd), 5′-CCT GGC TAT GTC ATT GCA ACA-3′; Insl3 (rev), 5′-TGG TCC TTG CTT ACT GCG ATC T-3′ [Cederroth et al., 2007]; and P450scc (fwd), 5′-CAG AAC TAA GAC CTG GAA GGA CCA-3′; P450scc (rev), 5′-TGG GTG TAC TCA TCA GCT TTA TTG AA-3′.

Results

Regression of Seminal Vesicles in Aged AhR(−/−) *Males*

We have previously reported that *AhR*(−/−) female mice had defective reproductive activity. In the present study, we examined the effect of *AhR* on the reproductive activity in *AhR*(−/−) males. Although the defect was milder than that observed in females, we found suppression of reproductive activity in aged *AhR*(−/−) males. Therefore, we examined whether the reproductive tissues are also affected in *AhR*(−/−) males. The seminal vesicle was completely regressed in certain population of *AhR*(−/−) males (fig. 1A). At the same time, we noticed that this tissue regression was rare in the young adult. Therefore, the regression was examined in terms of animal age. Regression of the seminal vesicle was identified in 53.8% of the 24-week-old, 66.7% of the 32-week-old, and 50.0% of the 52-week-old *AhR*(−/−) males, whereas no such regression was observed in the 8-week-old knockout males (fig. 1B). No such tissue regression was observed in age-matched *AhR*(+/+) mice, strongly suggesting that AhR is essential for the maintenance of seminal vesicle in aged mice.

Next, we quantified the regression process by measuring tissue weight. The weight of the seminal vesicles was similar in *AhR*(+/+) and *AhR*(−/−) at 8 weeks after birth (fig. 1C). However, the weight of the *AhR*(−/−) seminal vesicles did not increase after 24 weeks while that of *AhR*(+/+) increased in an age-dependent manner. We expected to observe apparent tissue regression in some of the knockout animals, but no such tissue was observed, suggesting that the regression occurs and is completed rapidly.

Since AhR is implicated in maintenance of the seminal vesicle, the expression of AhR in the seminal vesicle was analyzed by immunohistochemistry (fig. 1D) and Western blotting (fig. 2B). As shown in figure 1D, AhR was expressed in the epithelial cells of the seminal vesicle and accumulated in the cytoplasm rather than in the nuclei of these cells. This cytoplasmic localization was similar to that observed in the liver [Poland et al., 1976].

Testosterone Synthesis in AhR(−/−) *Males*

Since proliferation of the seminal vesicle epithelial cells is controlled by an androgen-mediated signal [Neubauer et al., 1981], we subsequently investigated the expression of androgen receptor (AR) immunohistochemically (fig. 2A). Similar to AhR, AR was expressed in the epithelial cells of the seminal vesicle. To assess whether regression of the seminal vesicle is due to low expression of AR in *AhR*(−/−) animal, whole tissue extracts were prepared from the seminal vesicles of *AhR*(+/+) and *AhR*(−/−) males at 8 and 32 weeks of age, and then subjected to Western blot analyses. Unexpectedly, however, no decrease in the expression of AR was observed in the absence of AhR at both 8 and 32 weeks (fig. 2B).

In addition to AR, testosterone is required for AR signaling. Therefore, we were interested in determining whether testosterone production is affected in *AhR*(−/−)

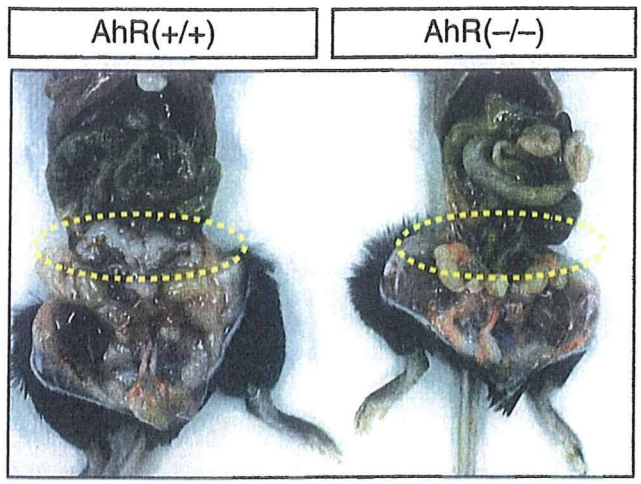

A

	AhR(+/+)	AhR(–/–)
8-week	5/5 (100%)	4/4 (100%)
24-week	8/8 (100%)	6/13 (46.2%)
32-week	4/4 (100%)	1/3 (33.3%)
52-week	8/8 (100%)	5/10 (50.0%)

B

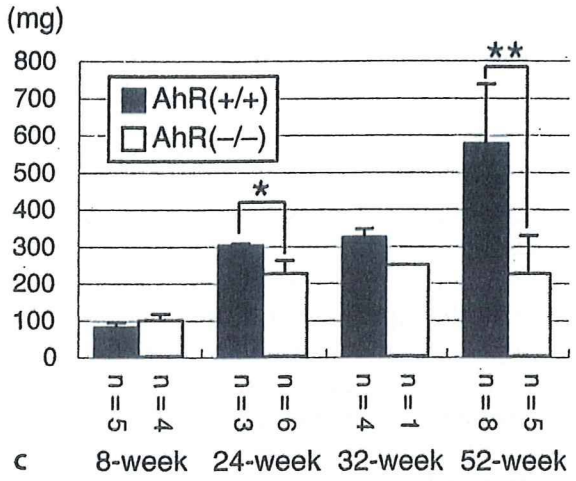

C

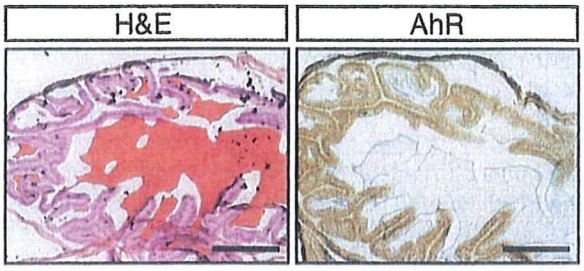

D

Fig. 1. Seminal vesicle regression in aged *AhR*(–/–) mice. **A** The reproductive tracts of 20-week-old *AhR*(+/+) and *AhR*(–/–) males. The seminal vesicle in the *AhR*(+/+) male is indicated by yellow dotted circles while this tissue is absent in the *AhR*(–/–) male. **B** Seminal vesicle regression in *AhR*(–/–) males is age-dependent. *AhR*(+/+) and *AhR*(–/–) males at 8, 24, 32, and 52 weeks of age were analyzed for the presence of seminal vesicles. Data are numbers of mice with intact seminal vesicles per total number of mice. **C** Comparison of seminal vesicle wet weight between *AhR*(+/+) and *AhR*(–/–) males. The seminal vesicles isolated from 8-, 24-, 32-, and 52-week-old *AhR*(+/+) and *AhR*(–/–) males were weighed. Numbers of the mice examined are indicated. Values are mean ± SD, * $p < 0.025$, ** $p < 0.005$. Statistical analysis was not performed with the 32-week-old mice because the number of *AhR*(–/–) males harboring the seminal vesicle was small. **D** Expression of AhR in the seminal vesicle. Ten-micrometer cryosections were prepared from a 10-week-old *AhR*(+/+) seminal vesicle. The sections were stained with hematoxylin and eosin (H&E) or immunohistochemically with anti-AhR antibody (AhR). Scale bars = 200 μm.

males. The testicular weight of *AhR*(–/–) males was compared with that of age-matched *AhR*(+/+) males at 8, 24, 32, and 52 weeks after birth. As shown in fig. 3A, the weights were mostly similar in *AhR*(+/+) and *AhR*(–/–) males at the above ages, although a slight difference was observed in 52-week-old mice. We then measured serum testosterone concentration in the 24- and 52-week-old mice, and found that it had clearly decreased in *AhR*(–/–) mice to approximately one third, and half of 24- and 52-week-old *AhR*(+/+) mice (fig. 3B). This result suggested that low testosterone concentrations cause, at least in part, the defect of seminal vesicles of aged *AhR*(–/–) males.

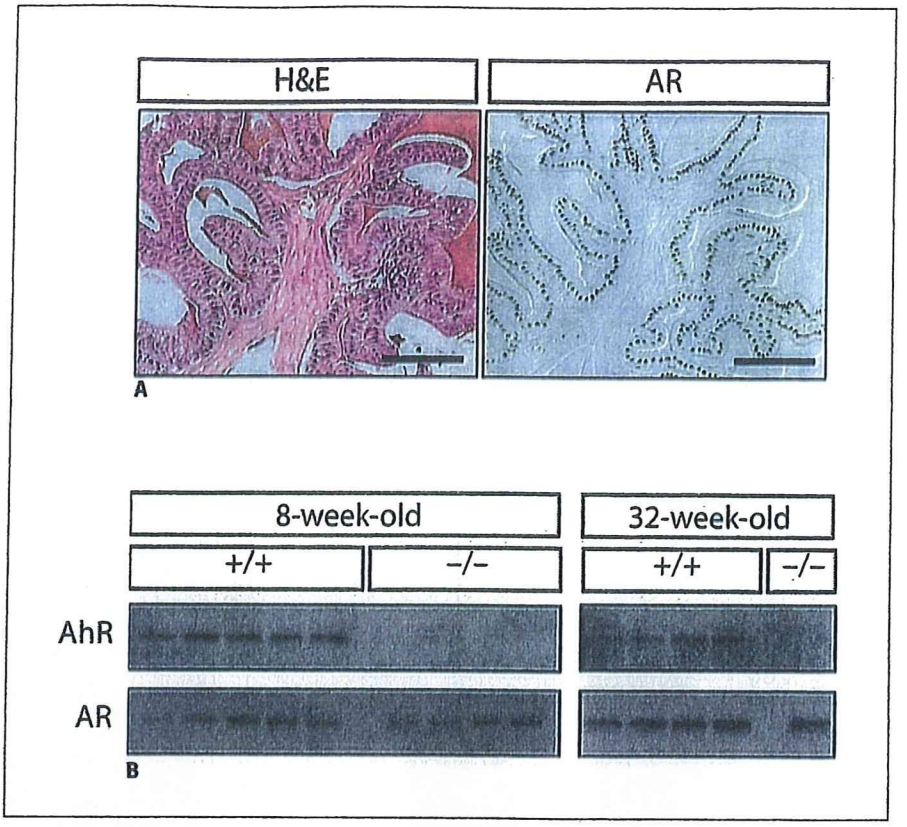

Fig. 2. Unaffected expression of androgen receptor in seminal vesicle of *AhR*(−/−). **A** Expression of AR in the seminal vesicle. Cryosections (10 μm thick) were prepared from seminal vesicles of 10-week-old *AhR*(+/+) and stained with hematoxylin and eosin (H&E) or anti-AR antibody (AR). Scale bars = 200 μm. **B** Expression of AR in seminal vesicles of 8- and 32-week-old *AhR*(+/+) and *AhR*(−/−) males. Whole tissue extracts (10 μg) prepared from seminal vesicles were subjected to Western blot analyses with antibodies for AhR and AR. Five 8-week-old *AhR*(+/+) seminal vesicles, four 8-week-old *AhR*(−/−) seminal vesicles, four 32-week-old *AhR*(+/+) seminal vesicles, and one 32-week-old *AhR*(−/−) seminal vesicle were used.

Since spermatogenesis is one of the physiological events in the testis and is regulated by testosterone, we also determined whether sperm production is affected in the *AhR*(−/−) testes. We counted epididymal sperm numbers in *AhR*(+/+) and (−/−) mice (fig. 3C). The number was decreased in the *AhR*(−/−) mice to approximately two thirds of the *AhR*(+/+), suggesting that low concentrations of serum testosterone affect spermatogenesis in the *AhR*(−/−) testes. To investigate the process of spermatogenesis, serial sections of the *AhR*(+/+) and *AhR*(−/−) testes were prepared. Morphologically, a substantial number of elongated spermatids were differentiated in the *AhR*(−/−) testes as well as *AhR*(+/+) testes (fig. 3D). Moreover, histological examination of the caudae epididymidis revealed the presence of abundant sperm cells even in the *AhR*(−/−) males. No evidence of any histological abnormality that would cause the reduced number of the sperm was observed in the *AhR*(−/−) testes.

Low Expression of 3βHsd in AhR(−/−) *Testes*

Testosterone is synthesized in testicular Leydig cells, and therefore coincident AhR expression was determined in Leydig cells. Consistent with previous reports [Schultz et al., 2003], anti-AhR immunoreactivity was detected in Leydig cells (fig. 4A). The low serum testosterone concentration suggested the potential involvement of AhR in the development and/or function of Leydig cells. Therefore, we performed immunohistochemical staining with antibody for 3βHsd, a Leydig cell marker [Dupont et al., 1990]. As shown in figure 4A, Leydig cells were present in the testes of both genotypes. We then performed fluorescent immunohistochemical examination followed by cell counting to determine if the number of Leydig cells is decreased in the *AhR*(−/−) testes (fig. 4B). There was no significant difference in Leydig cell number between the testes of *AhR*(+/+) and *AhR*(−/−) (fig. 4C), suggesting that the low level of serum testosterone is not due to a decrease in Leydig cell number but rather reduced ability to produce testosterone. To investigate the possibility of suppression of steroidogenic function of Leydig cells, we compared the expression of 3βHsd in *AhR*(+/+) and *AhR*(−/−) testes by Western blot analyses. Comparable expression of 3βHsd was observed in 10-week-old *AhR*(+/+) and *AhR*(−/−) mice, but the expression was less in 24-, 32-, and 52-week-old *AhR*(−/−) testes compared to age-matched *AhR*(+/+) mice (fig. 5A).

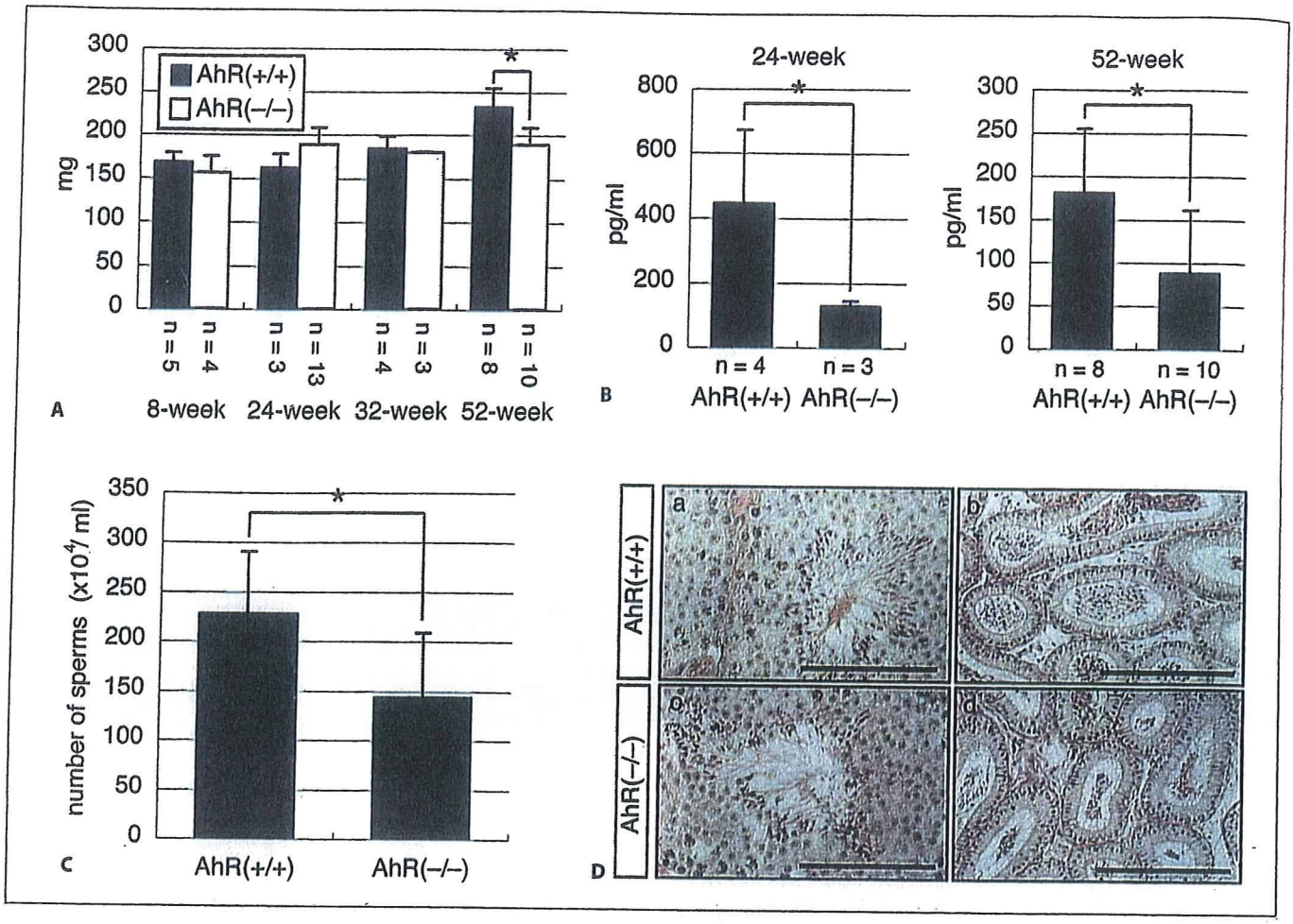

Fig. 3. Low serum testosterone levels in *AhR*(–/–) males. **A** Comparison of testicular weight between *AhR*(+/+) and *AhR*(–/–) mice. The testes isolated from 8-, 24-, 32-, and 52-week-old *AhR*(+/+) and *AhR*(–/–) mice were weighed. Numbers of mice examined are indicated. Values are mean ± SD, * $p < 0.005$. **B** Serum testosterone concentrations in 24- and 52-week-old *AhR*(+/+) and *AhR*(–/–) mice determined by enzymatic immunoassay. Numbers of mice examined are indicated. Values are mean ± SD, * $p < 0.05$. **C** Comparison of epididymal sperm number between 52-week-old *AhR*(+/+) and *AhR*(–/–). Sperm cells were recovered from eight *AhR*(+/+) and ten *AhR*(–/–) 52-week-old mice. * $p < 0.025$. **D** Histological analysis of the testes (**a**, **c**) and caudae epididymidis (**b**, **d**) of *AhR*(+/+) and *AhR*(–/–) mice. Five-micrometer paraffin-embedded sections of the testes and caudae epididymidis from 20-week-old *AhR*(+/+) and *AhR*(–/–) mice were stained with hematoxylin and eosin. Scale bars in **a** and **c** = 100 μm, **b** and **d** = 200 μm.

Our previous study demonstrated that AhR regulates *Cyp19* (aromatase P450) gene expression in the ovary [Baba et al., 2005]. Since aromatase P450 is capable of converting testosterone to estradiol, increased expression of the enzyme would lead to decrease in serum testosterone and thus Cyp19 expression was examined in 24-week-old mice. However, there was no discernible difference in Cyp19 expression between the *AhR*(+/+) and *AhR*(–/–) testes (fig. 5B). Moreover, the expression of StAR (steroidogenic acute regulatory protein), Insl3 (insulin like-3), and P450scc (side chain cleavage) necessary for the endocrine function of Leydig cells was examined by quantitative RT-PCR. As shown in figure 5C, the expression of the *StAR* gene was decreased as well as *3βHsd* in the *AhR*(–/–) testes. In contrast, the expression of *Insl3* and *P450scc* in the *AhR*(–/–) testes was comparable to *AhR*(+/+), indicating that not all the steroidogenic genes are regulated by AhR. Further, we investigated the expression of Ad4BP/SF-1, which is known to regulate the expression of all steroidogenic genes; however, the expression of Ad4BP/SF-1 protein was not affected in the *AhR*(–/–) testes (fig. 5D).

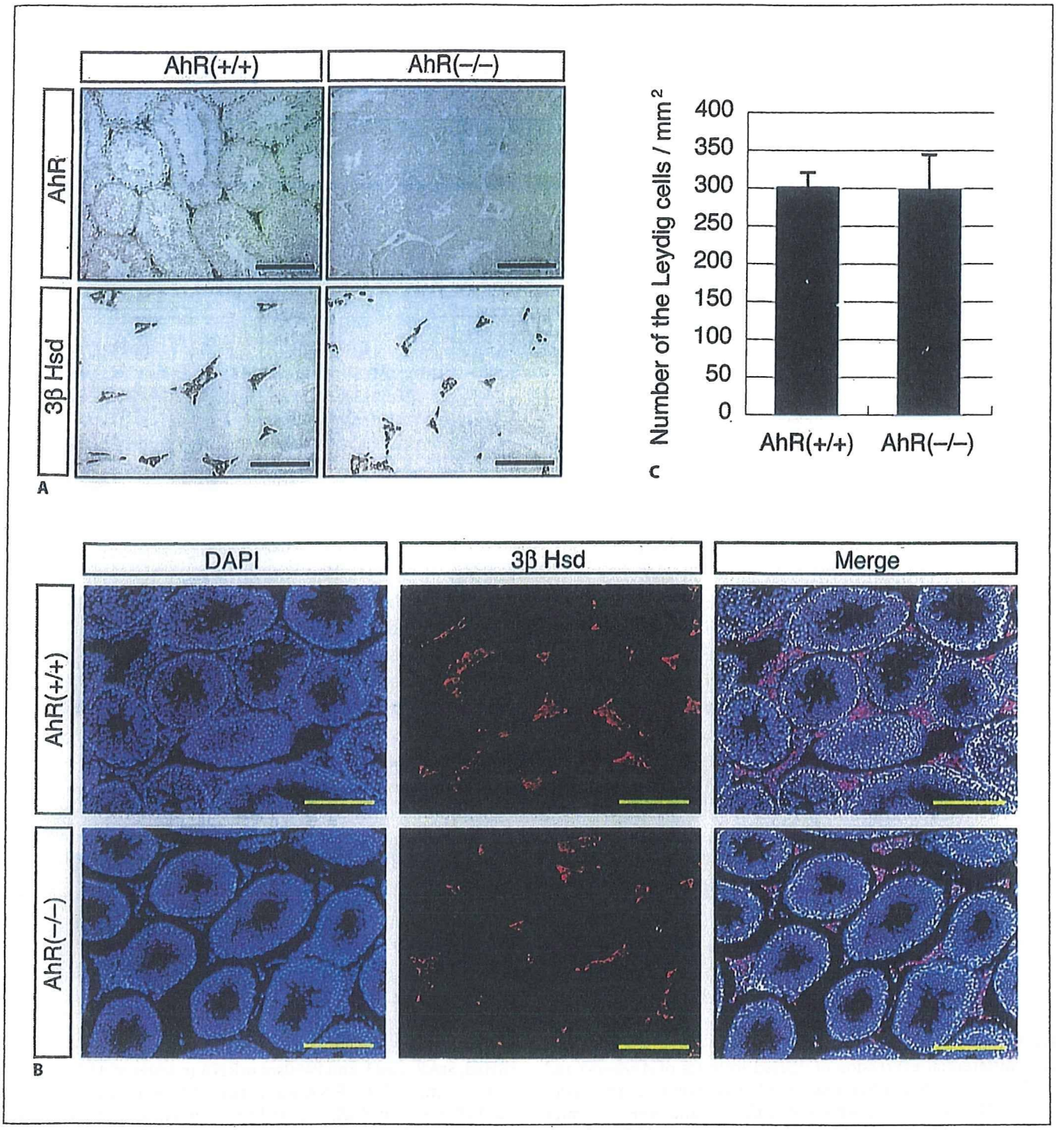

Fig. 4. No difference in number of testicular Leydig cells between *AhR*(+/+) and *AhR*(–/–) mice. **A** Expression of AhR and 3βHsd in Leydig cells. Five-micrometer paraffin sections were prepared from the testes of 24-week-old *AhR*(+/+) and *AhR*(–/–) mice and subjected to immunohistochemical analyses using anti-AhR and anti-3βHsd antibodies. Scale bars = 200 μm. **B** Immunohistochemical staining of testes of 52-week-old *AhR*(+/+) and *AhR*(–/–) mice using anti-3βHsd antibody (red). Nuclei were stained with DAPI (blue). Sections were prepared from eight *AhR*(+/+) and ten *AhR*(–/–) mice. Representative results are shown. Scale bars = 200 μm. **C** Comparison of Leydig cell number between *AhR*(+/+) and *AhR*(–/–). Numbers of 3βHsd-positive cells in testes of eight *AhR*(+/+) and ten *AhR*(–/–). 3βHsd-positive cells were counted in four sections for each animal. Values are average numbers of Leydig cells ± SD per mm².

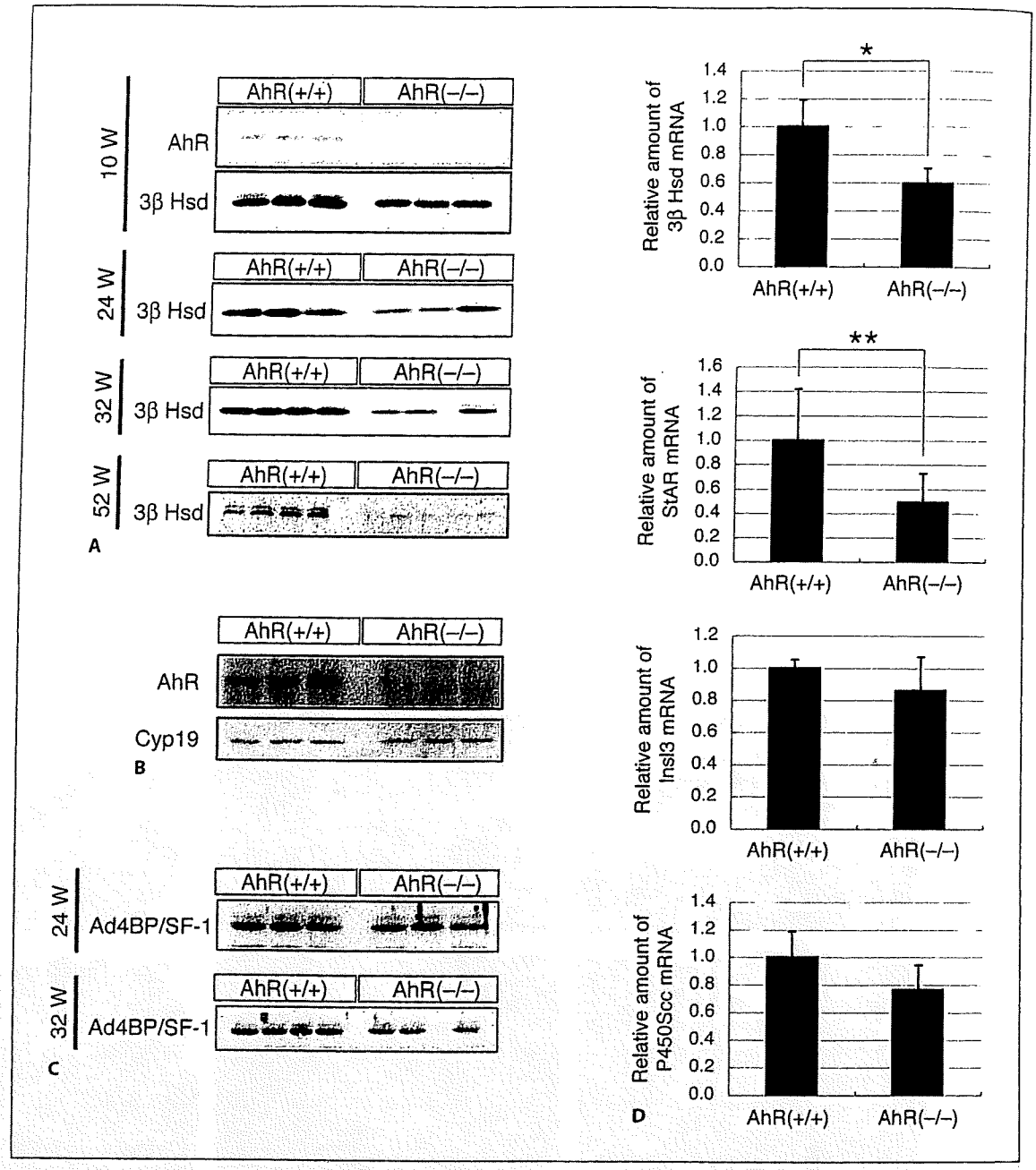

Fig. 5. Low expression of 3βHsd in *AhR*(–/–) testes. **A** Age-dependent differential expression of 3βHsd in testes of *AhR*(+/+) and *AhR*(–/–) mice. Whole tissue extracts (10 μg) prepared from testes of 10-, 24-, 32-, and 52-week-old *AhR*(+/+) and *AhR*(–/–) mice were subjected to Western blot analyses using anti-AhR and anti-3βHsd antibodies. Three or four males were used for each blotting. **B** Expression of Cyp19 in testes of *AhR*(+/+) and *AhR*(–/–) mice. Whole tissue extracts (10 μg) prepared from testes of 24-week-old *AhR*(+/+) and *AhR*(–/–) mice were subjected to Western blot analyses using anti-AhR and anti-Cyp19 antibodies. Three *AhR*(+/+) and three *AhR*(–/–) males were used. **C** Expression of 3βHsd, StAR, Insl3, and P450scc mRNA in testes of *AhR*(+/+) and *AhR*(–/–) mice. Total RNA was prepared from testes of 52-week-old *AhR*(+/+) and *AhR*(–/–), and then the amount of the mRNA was quantified by real-time RT-PCR, * $p < 0.025$, ** $p < 0.1$. **D** Expression of Ad4BP/SF-1 in testes of *AhR*(+/+) and *AhR*(–/–) mice. Whole tissue extracts (10 μg) prepared from testes of 24- and 32-week-old *AhR*(+/+) and *AhR*(–/–) mice were subjected to Western blot analyses using anti-Ad4BP/SF-1 antibodies. Three *AhR*(+/+) and three *AhR*(–/–) males were used.

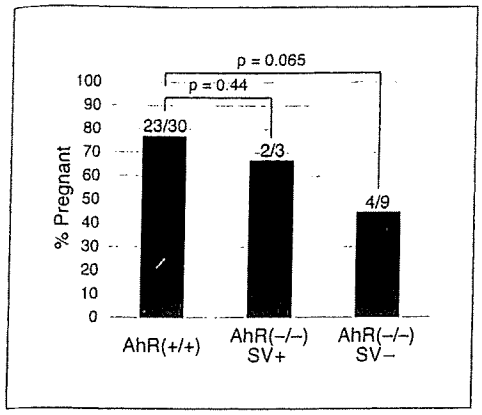

Fig. 6. Low fertility of *AhR*(−/−) males lacking seminal vesicles. Thirty *AhR*(+/+) and three *AhR*(−/−) mice with seminal vesicles, and nine *AhR*(−/−) mice lacking seminal vesicles were mated with *AhR*(+/+) females. Data represent the percentages of successful pregnancies. Numbers on bars represent the number of pregnant females per total number of female mice.

Reduced Fertility of AhR(−/−) *Males*

Lastly, we examined how the reproductive activity is affected in *AhR*(−/−) males. In order to determine reproductive activity, 21- to 33-week-old *AhR*(+/+) and *AhR*(−/−) males were mated with wild-type females. Before mating, the *AhR*(−/−) males were surgically examined to determine whether they still possess the seminal vesicles or not. Three of these males still had their seminal vesicles while nine of them did not. These two groups, together with wild-type males, were then subjected to mating experiments. *AhR*(−/−) males lacking any seminal vesicles showed less reproductive activity than *AhR*(+/+) males and *AhR*(−/−) males harboring the seminal vesicle (fig. 6). The reproductive activity of *AhR*(−/−) males harboring seminal vesicles was not statistically different from that of *AhR*(+/+) males (fig. 6).

During this experiment, the presence of seminal vaginal plugs was checked every morning, and frequently these plugs showed abnormal characteristics with the female mice mated with the *AhR*(−/−) males. Small amounts of white-colored and non-fixed plugs were observed in females mated with males lacking the seminal vesicles (data not shown). Since the vaginal plug is considered to be critical for successful pregnancy, the rate of pregnancy was compared between females with normal and those with abnormal plugs. As expected, successful pregnancies were counted in 4 of the 5 females with normal plugs, while 5 of the 6 females with the abnormal plug had unsuccessful pregnancies.

Discussion

Through the analyses of *AhR*(−/−) males, we demonstrated a novel function for AhR: maintenance of the seminal vesicle. Although the weight of the seminal vesicle was reported previously to be decreased by *AhR* gene disruption [Lin et al., 2002], we showed for the first time a complete regression of the seminal vesicle in *AhR*(−/−) males. At the same time, we noticed that the regression occurs preferentially in aged adult animals. Since the previous study only examined mice that were younger than 90 days old [Lin et al., 2002], it seems perhaps unlikely to encounter any mice lacking the seminal vesicle at that young age. In order to explain the mechanism underlying tissue regression, it was important to examine if apoptosis is increased while cell proliferation is decreased during and just prior to the regression. However, since this regression is considered to occur randomly among individuals, we could not find seminal vesicles in which regression was apparently in progress, suggesting that the process of regression proceeds in a very short period. Because of this regression feature, we neither can predict precisely when the regression starts in each animal, nor determine whether this regression is caused by increased apoptosis or decreased cell proliferation.

Developmentally, the seminal vesicle is derived from the caudal region of the Wolffian duct as a male sex-accessory gland. Likewise, the coagulating gland is derived from the same duct, and thereafter it is fused to the posterior margin of the seminal vesicle. Therefore, the coagulating gland may disappear simultaneously with the seminal vesicle in *AhR*(−/−) males. Functionally, the coagulating gland secretes a substance required for the formation of a vaginal plug to guarantee efficient pregnancies. In this study, we observed a decrease in successful reproductive activity and abnormal vaginal plugs when *AhR*(−/−) males were used in the mating. Therefore, we assumed that the abnormal vaginal plug formation caused by the disappearance of the seminal vesicle together with coagulating gland is a possible reason accounting for the decreased reproductive activity of *AhR*(−/−) males. In addition to vaginal plug formation, sperm number is another factor to guarantee efficient pregnancies. Therefore, we counted the number of epididymal sperms and found that it was reduced in *AhR*(−/−). Although a definite relationship between fertility and sperm number has yet to be determined, this observation raises another possibility: the low sperm count explains the decreased reproductive activity of *AhR*(−/−) males.

The implication of AR in seminal vesicle development was elucidated by *Ar*-knockout mice in which the seminal vesicles failed to develop from the fetal stage [De Gendt et al., 2004]. In addition, castration at adulthood led to regression of the seminal vesicle while administration of dihydrotestosterone rescued such castration-induced regression [Neubauer et al., 1981]. Moreover, administration of androgen antagonists decreased the weight of the seminal vesicle [Vinggaard et al., 2002]. These observations indicated that androgen signaling is indispensable for the maintenance of the adult seminal vesicle as well as for the development of fetal tissue. Considering the importance of androgen signaling in the development and maintenance of the seminal vesicle, we reasoned two possibilities for tissue regression; one is the low expression of AR in the seminal vesicle while the other is reduced testosterone production in testicular Leydig cells. Since AhR is expressed in both seminal vesicles and Leydig cells, any disruption of the *AhR* gene would potentially affect both or either of them. Eventually, examination of the two possibilities strongly suggested that the decreased expression of 3βHsd and StAR in testicular Leydig cells leads to a concomitant decrease in serum testosterone and thus the regression of the seminal vesicle in the *AhR*(–/–) male. Androgen is known to mediate a variety of male functions, and spermatogenesis is one representative event. In fact, sperm production was affected in *AhR*(–/–) males. This differential tissue effect in the decrease of testosterone is possibly due to the sensitivity to testosterone concentration. In fact, administration of androgen antagonist demonstrated that the seminal vesicle is the most sensitive tissue among the male reproductive accessory tissues [Vinggaard et al., 2002].

The expression of AhR in the seminal vesicle implies specific functions of this receptor in the tissue. Although AhR does not regulate AR expression, AhR possibly regulates genes essential for the proliferation of seminal vesicle epithelial cells. In fact, an AhR-defective variant of mouse hepatoma Hepa 1c1c7 cells exhibited a prolonged doubling time caused by G_1 cell-cycle arrest [Ma and Whitlock, 1996]. Embryonic fibroblasts prepared from *AhR*(–/–) tissue grow slower because of accumulation of cells in G_2/M-phase due to an altered expression of G_2/M kinases Cdc2 and Plk [Elizondo et al., 2000]. These observations suggest that AhR promotes cell proliferation. However, opposing functions of AhR in cell cycle regulation have also been demonstrated. For example, in rat 5L hepatoma cells, G_1 arrest was induced by TCDD, an AhR ligand, which resulted in overexpression of CDK2 inhibitor, $P27^{kip1}$ [Kolluri et al., 1999; Sherr and Roberts, 1999]. It was also revealed that AhR forms a protein-protein complex with RB [Ge and Elferink, 1998; Puga et al., 2000; Elferink et al., 2001]. Taken together, it has been well-established that AhR regulates cell proliferation. Thus, in addition to the non-cell-autonomous effects observed in response to decreased testosterone production, the seminal vesicle is potentially regressed cell-autonomously through an abnormal cell cycle regulation in *AhR*(–/–) cells.

Our study demonstrated that the seminal vesicle regressed in the aged *AhR*(–/–) males and that this regression is likely caused by a decrease in testosterone production. In fact, low expression levels of 3βHsd and StAR were found in the *AhR*(–/–) testes. Likewise, our previous study [Baba et al., 2005] demonstrated that AhR activates aromatase *P450* (*Cyp19*) gene transcription in the steroidogenic granulosa cells when the ovaries are at preovulatory phase in the estrous cycle [Lynch et al., 1993]. However, no alteration of Cyp19 expression was observed in the *AhR*(–/–) testes. These results clearly demonstrated that AhR is involved in sex steroid synthesis in both sexes although the affected sites in the steroidogenic process are different between males and females. The mechanism for the sex differences in AhR action remains to be resolved, however, these observations strongly suggested that, similar to the female reproductive activity, AhR has a critical function in the male reproduction as well.

Acknowledgements

We like to thank Dr. R.S. Pollenz (University of South Florida) and Dr. N. Harada (Fujita Health University) for kindly providing the anti-AhR antibody and anti-Cyp19 antibody, respectively. We are also grateful to Ms. M. Sugiura and Mrs. Y. Nemoto for their clerical assistance. This work was funded in part by Core Research for Evolutionary Science and Technology, Solution Oriented Research for Science and Technology from Japan Science and Technology and Research Fellowship (T. Baba) of the Japan Society for the Promotion of Science for Young Scientists.

References

Baba T, Mimura J, Nakamura N, Harada N, Yamamoto M, Morohashi K, Fujii-Kuriyama Y: Intrinsic function of the aryl hydrocarbon (dioxin) receptor as a key factor in female reproduction. Mol Cell Biol 25:10040–10051 (2005).

Bell DR, Clode S, Fan MQ, Fernandes A, Foster PM, et al: Toxicity of 2,3,7,8-tetrachlorodibenzo-p-dioxin in the developing male Wistar(Han) rat. II: Chronic dosing causes developmental delay. Toxicol Sci 99:224–233 (2007).

Brown NM, Manzolillo PA, Zhang JX, Wang J, Lamartiniere CA: Prenatal TCDD and predisposition to mammary cancer in the rat. Carcinogenesis 19:1623–1629 (1998).

Burbach KM, Poland A, Bradfield CA: Cloning of the Ah-receptor cDNA reveals a distinctive ligand-activated transcription factor. Proc Natl Acad Sci USA 89:8185–8189 (1992).

Cederroth CR, Schaad O, Descombes P, Chambon P, Vassalli JD, Nef S: Estrogen receptor alpha is a major contributor to estrogen-mediated fetal testis dysgenesis and cryptorchidism. Endocrinology 148:5507–5519 (2007).

Cooke PS, Young P, Cunha GR: Androgen receptor expression in developing male reproductive organs. Endocrinology 128:2867–2873 (1991).

Cunha GR: Epithelio-mesenchymal interactions in primordial gland structures which become responsive to androgenic stimulation. Anat Rec 172:179–195 (1972).

Curtis Hewitt S, Goulding EH, Eddy EM, Korach KS: Studies using the estrogen receptor alpha knockout uterus demonstrate that implantation but not decidualization-associated signaling is estrogen dependent. Biol Reprod 67:1268–1277 (2002).

De Gendt K, Swinnen JV, Saunders PT, Schoonjans L, Dewerchin M, et al: A Sertoli cell-selective knockout of the androgen receptor causes spermatogenic arrest in meiosis. Proc Natl Acad Sci USA 101:1327–1332 (2004).

Dupont E, Zhao HF, Rheaume E, Simard J, Luu-The V, Labrie F, Pelletier G: Localization of 3 beta-hydroxysteroid dehydrogenase/delta 5-delta 4-isomerase in rat gonads and adrenal glands by immunocytochemistry and in situ hybridization. Endocrinology 127:1394–1403 (1990).

Dupont S, Krust A, Gansmuller A, Dierich A, Chambon P, Mark M: Effect of single and compound knockouts of estrogen receptors alpha (ERalpha) and beta (ERbeta) on mouse reproductive phenotypes. Development 127:4277–4291 (2000).

Elferink CJ, Ge NL, Levine A: Maximal aryl hydrocarbon receptor activity depends on an interaction with the retinoblastoma protein. Mol Pharmacol 59:664–673 (2001).

Elizondo G, Fernandez-Salguero P, Sheikh MS, Kim GY, Fornace AJ, Lee KS, Gonzalez FJ: Altered cell cycle control at the G(2)/M phases in aryl hydrocarbon receptor-null embryo fibroblast. Mol Pharmacol 57:1056–1063 (2000).

Ema M, Sogawa K, Watanabe N, Chujoh Y, Matsushita N, et al: cDNA cloning and structure of mouse putative Ah receptor. Biochem Biophys Res Commun 184:246–253 (1992).

Fisher CR, Graves KH, Parlow AF, Simpson ER: Characterization of mice deficient in aromatase (ArKO) because of targeted disruption of the *cyp19* gene. Proc Natl Acad Sci USA 95:6965–6970 (1998).

Fujisawa-Sehara A, Sogawa K, Yamane M, Fujii-Kuriyama Y: Characterization of xenobiotic responsive elements upstream from the drug-metabolizing cytochrome P-450c gene: a similarity to glucocorticoid regulatory elements. Nucleic Acids Res 15:4179–4191 (1987).

Ge NL, Elferink CJ: A direct interaction between the aryl hydrocarbon receptor and retinoblastoma protein. Linking dioxin signaling to the cell cycle. J Biol Chem 273:22708–22713 (1998).

Gibbons A: Dioxin tied to endometriosis. Science 262:1373 (1993).

Gray LE Jr, Kelce WR, Monosson E, Ostby JS, Birnbaum LS: Exposure to TCDD during development permanently alters reproductive function in male Long Evans rats and hamsters: reduced ejaculated and epididymal sperm numbers and sex accessory gland weights in offspring with normal androgenic status. Toxicol Appl Pharmacol 131:108–118 (1995).

Hahn ME: Aryl hydrocarbon receptors: diversity and evolution. Chem Biol Interact 141:131–160 (2002).

Hankinson O: The aryl hydrocarbon receptor complex. Annu Rev Pharmacol Toxicol 35:307–340 (1995).

Kolluri SK, Weiss C, Koff A, Gottlicher M: p27(Kip1) induction and inhibition of proliferation by the intracellular Ah receptor in developing thymus and hepatoma cells. Genes Dev 13:1742–1753 (1999).

Lahvis GP, Pyzalski RW, Glover E, Pitot HC, McElwee MK, Bradfield CA: The aryl hydrocarbon receptor is required for developmental closure of the ductus venosus in the neonatal mouse. Mol Pharmacol 67:714–720 (2005).

Lin TM, Ko K, Moore RW, Simanainen U, Oberley TD, Peterson RE: Effects of aryl hydrocarbon receptor null mutation and in utero and lactational 2,3,7,8-tetrachlorodibenzo-p-dioxin exposure on prostate and seminal vesicle development in C57BL/6 mice. Toxicol Sci 68:479–487 (2002).

Lynch JP, Lala DS, Peluso JJ, Luo W, Parker KL, White BA: Steroidogenic factor 1, an orphan nuclear receptor, regulates the expression of the rat aromatase gene in gonadal tissues. Mol Endocrinol 7:776–786 (1993).

Ma Q, Whitlock JP Jr: The aromatic hydrocarbon receptor modulates the Hepa 1c1c7 cell cycle and differentiated state independently of dioxin. Mol Cell Biol 16:2144–2150 (1996).

Mimura J, Fujii-Kuriyama Y: Functional role of AhR in the expression of toxic effects by TCDD. Biochim Biophys Acta 1619:263–268 (2003).

Mimura J, Yamashita K, Nakamura K, Morita M, Takagi TN, et al: Loss of teratogenic response to 2,3,7,8-tetrachlorodibenzo-p-dioxin (TCDD) in mice lacking the Ah (dioxin) receptor. Genes Cells 2:645–654 (1997).

Morohashi K, Zanger UM, Honda S, Hara M, Waterman MR, Omura T: Activation of CYP11A and CYP11B gene promoters by the steroidogenic cell-specific transcription factor, Ad4BP. Mol Endocrinol 7:1196–1204 (1993).

Morohashi K, Iida H, Nomura M, Hatano O, Honda S, et al: Functional difference between Ad4BP and ELP, and their distributions in steroidogenic tissues. Mol Endocrinol 8:643–653 (1994).

Neubauer B, Blume C, Cricco R, Greiner J, Mawhinney M: Comparative effects and mechanisms of castration, estrogen anti-androgen, and anti-estrogen-induced regression of accessory sex organ epithelium and muscle. Invest Urol 18:229–234 (1981).

Poland A, Knutson JC: 2,3,7,8-tetrachlorodibenzo-p-dioxin and related halogenated aromatic hydrocarbons: examination of the mechanism of toxicity. Annu Rev Pharmacol Toxicol 22:517–554 (1982).

Poland A, Glover E, Kende AS: Stereospecific, high affinity binding of 2,3,7,8-tetrachlorodibenzo-p-dioxin by hepatic cytosol. Evidence that the binding species is receptor for induction of aryl hydrocarbon hydroxylase. J Biol Chem 251:4936–4946 (1976).

Puga A, Barnes SJ, Dalton TP, Chang C, Knudsen ES, Maier MA: Aromatic hydrocarbon receptor interaction with the retinoblastoma protein potentiates repression of E2F-dependent transcription and cell cycle arrest. J Biol Chem 275:2943–2950 (2000).

Schultz R, Suominen J, Varre T, Hakovirta H, Parvinen M, Toppari J, Pelto-Huikko M: Expression of aryl hydrocarbon receptor and aryl hydrocarbon receptor nuclear translocator messenger ribonucleic acids and proteins in rat and human testis. Endocrinology 144:767–776 (2003).

Sherr CJ, Roberts JM: CDK inhibitors: positive and negative regulators of G1-phase progression. Genes Dev 13:1501–1512 (1999).

Shimizu Y, Nakatsuru Y, Ichinose M, Takahashi Y, Kume H, et al: Benzo[a]pyrene carcinogenicity is lost in mice lacking the aryl hydrocarbon receptor. Proc Natl Acad Sci USA 97:779–782 (2000).

Sommer RJ, Ippolito DL, Peterson RE: In utero and lactational exposure of the male Holtzman rat to 2,3,7,8-tetrachlorodibenzo-p-dioxin: decreased epididymal and ejaculated sperm numbers without alterations in sperm transit rate. Toxicol Appl Pharmacol 140:146–153 (1996).

Vinggaard AM, Nellemann C, Dalgaard M, Jorgensen EB, Andersen HR: Antiandrogenic effects in vitro and in vivo of the fungicide prochloraz. Toxicol Sci 69:344–353 (2002).

ARTHRITIS & RHEUMATISM
Vol. 58, No. 2, February 2008, pp 389–400
DOI 10.1002/art.23163

Effective Treatment With Oral Administration of Rebamipide in a Mouse Model of Sjögren's Syndrome

Masayuki Kohashi,[1] Naozumi Ishimaru,[2] Rieko Arakaki,[2] and Yoshio Hayashi[2]

Objective. **To determine whether oral administration of rebamipide, a mucosal protective agent, is effective in the treatment of Sjögren's syndrome (SS) in the NFS/*sld* mouse model of the disease.**

Methods. **NFS/*sld* mice were given daily oral doses of rebamipide (0.3 mg/kg of body weight or 3 mg/kg) or vehicle alone starting from the age of 4 weeks to the age of 8 weeks. The volume of saliva and tears was monitored during and after treatment. After the final dose, histologic features of the tissues, TUNEL+ apoptotic duct cells in affected glands, T cell and cytokine function, and levels of immunoglobulin isotypes and serum autoantibodies were examined.**

Results. **The 3-mg/kg dose of rebamipide prevented the development of autoimmune lesions. The average volume of saliva in rebamipide-treated mice was significantly higher than that in control mice. We found decreased TUNEL+ apoptotic duct cells in the salivary and lacrimal glands of rebamipide-treated mice as compared with control mice. Rebamipide treatment suppressed the activation of CD4+ T cells and Th1 cytokines (interleukin-2, interferon-γ) associated with impaired NF-κB activity. Production of serum autoantibodies, IgM, and IgG1 was clearly inhibited.**

Conclusion. **Our findings demonstrate the efficacy of oral administration of rebamipide in the treatment of SS. Rebamipide represents a new therapeutic strategy for the treatment of patients with sicca symptoms caused by SS, as well as for patients with other diseases.**

Sjögren's syndrome (SS) is an autoimmune disorder characterized by lymphocytic infiltrates and destruction of the salivary and lacrimal glands, as well as systemic production of autoantibodies to the RNP particles SSA/Ro and SSB/La (1–3). Although the specificity of cytotoxic T lymphocyte function has been an important issue in studies of organ-specific autoimmune responses, the mechanisms responsible for tissue destruction in SS remain to be fully elucidated. The immune system has acquired regulatory mechanisms that preclude the reactivity of mature T cells to self antigens presented by major histocompatibility complex (MHC) molecules, while maintaining an ability to respond to non-self antigens presented by self MHC molecules (4,5). The dysregulation of T cell tolerance is considered to be responsible for many types of autoimmune diseases, and a variety of mechanisms involved in the initiation of autoimmune diseases have been proposed (6–10).

Data from our previous studies demonstrated that autoreactive CD4+ T cells play a pivotal role in the development of autoimmune exocrinopathy in the NFS/*sld* mouse model of SS (11). It is now evident that the interaction of Fas with FasL regulates a large number of pathophysiologic processes of apoptosis, including autoimmune diseases (11,12). Previous studies have also confirmed the observation that apoptotic cells in various cell types are implicated as the source of autoantigen when stimulated with different proapoptotic stimuli (13).

On the other hand, natural autoantibody appears to be primarily IgM polyreactive antibody of low affinity, which is quite different from the monospecific high-affinity IgG antibody usually associated with autoimmune disease (14). It is important to note that au-

Supported in part by the Ministry of Education, Science, Sports, and Culture of Japan (Grants-in-Aid for Scientific Research 17109016 and 17689049) and the Uehara Memorial Foundation.

[1]Masayuki Kohashi, PhD: University of Tokushima Graduate School, and Otsuka Pharmaceutical Company, Ltd., Tokushima, Japan; [2]Naozumi Ishimaru, DDS, PhD, Rieko Arakaki, PhD, Yoshio Hayashi, DDS, PhD: University of Tokushima Graduate School, Tokushima, Japan.

Address correspondence and reprint requests to Yoshio Hayashi, DDS, PhD, Department of Oral Molecular Pathology, Institute of Health Biosciences, University of Tokushima Graduate School, 3 Kuramoto-cho, Tokushima 770-8504, Japan. E-mail: hayashi@dent.tokushima-u.ac.jp.

Submitted for publication June 15, 2007; accepted in revised form October 26, 2007.

toantigens released from the intracytoplasmic environment will not, under normal conditions, stimulate the production of pathogenic IgG autoantibodies capable of causing tissue damage (14,15). During an autoimmune disease, levels of IgM autoantibodies are high (16) due to the stimulation of IgM autoantibody–producing cell lines by the release of autoantigens from target cells. IgG antibodies are the primary mediators of protective humoral immunity against pathogens, but they can also be pathogenic. Acting as cytotoxic molecules or as immune complexes, IgG autoantibodies are the principal mediators of autoimmune diseases such as idiopathic thrombocytopenia, autoimmune hemolytic anemia, and systemic lupus erythematosus, and may contribute to other autoimmune diseases, such as rheumatoid arthritis, type 1 diabetes mellitus, and multiple sclerosis (17).

Rebamipide (2-[4-chlorobenzoylamino]-3-[2(1*H*)quinolinon-4-yl]propionic acid; OPC-12759) is a mucosal protective agent used for the treatment of gastritis and gastric ulcer. It has recently been reported that rebamipide works as an antiinflammatory agent in both acute and chronic inflammation and has an inhibitory effect on proinflammatory cytokines (18). Experimental data have shown that rebamipide can prevent Dextran sulfate sodium–induced colitis in rats (19). A recent study demonstrated the protective effect of rebamipide on the intestinal barrier, namely, its ability to reinforce the epithelial barrier capacity and to decrease macromolecular transport across this barrier (20). At the same time, the study demonstrated the immunoregulatory properties of rebamipide, which is capable of regulating lymphocyte proliferation and cytokine secretion (20).

The aim of the present study was to investigate the effects of oral administration of rebamipide on various parameters of autoimmune responses and on serum levels of autoantibodies, immunoglobulins, and inflammatory cytokines in a murine model of SS. We hypothesized that in this model of SS, the immunomodulatory activity of rebamipide against autoimmune responses to tissue-specific autoantigens would be a good therapeutic approach.

MATERIALS AND METHODS

Mice and experimental design. Female mice of the NFS/N strain carrying the mutant gene *sld* (21) were reared in our specific pathogen–free mouse colony and given food and water ad libitum. Thymectomy was performed on day 3 after birth in the NFS/*sld* mice (22). A total of 35 NFS/*sld* mice that had been subjected to thymectomy on day 3 after birth were investigated in the present study. An additional group of 10 mice not subjected to thymectomy were also investigated. Rebamipide (Otsuka Pharmaceutical, Tokushima, Japan) was prepared as a suspension in 0.5% carboxymethylcellulose (Dai-Ichi Chemical Industries, Tokyo, Japan) in water.

The following experimental groups were studied: a vehicle-treated control group, which received oral administration of vehicle alone (n = 12), and 2 rebamipide-treated groups, which received oral administration of rebamipide at a dose of either 0.3 mg/kg of body weight (n = 12) or 3 mg/kg of body weight (n = 11). Thymectomized NFS/*sld* mice were given daily oral treatment with rebamipide or vehicle, starting from the age of 4 weeks to age 8 weeks. Nonthymectomized mice (n = 10) received oral administration of vehicle alone.

OT-2 mice (C57BL/6-Tg[TcraTcrb]452Cbn/J) were obtained from Dr. J. Sprent (Garvan Institute of Medical Research, Darlinghurst, New South Wales, Australia). These mice (n = 5) were used in the transfer experiment.

All experiments were approved by the Animal Ethics Board of the University of Tokushima.

Histologic assessment. At the end of the treatment period, all organs were removed from the mice, fixed in 4% phosphate buffered formaldehyde (pH 7.2), and prepared for histologic examination. Formalin-fixed tissue sections were stained with hematoxylin and eosin, and 3 pathologists (NI, RA, and YH) independently evaluated the histologic features without knowledge of the condition of each mouse. Histologic changes were scored on a scale of 1–3, where 1 = no change or slight lymphoid cell infiltration (slight), 2 = mild lymphoid cell infiltration (moderate), and 3 = marked lymphoid cell infiltration with tissue destruction (severe). Histologic evaluation was performed in a blinded manner, and 1 tissue section from each salivary and lacrimal gland was evaluated.

TUNEL assay. Apoptotic cells were detected in tissue sections using the in situ TUNEL kit (Wako Pure Chemical, Osaka, Japan), as previously described (23). Briefly, sections were incubated with proteinase K (400 mg/ml) for 5 minutes, and then presoaked for 10 minutes in terminal deoxynucleotidyl transferase (TdT) buffer (0.5 μmoles/liter of cacodylate, 1 mmole/liter of $CoCl_2$, 0.5 μmoles/liter of dithiothreitol, 0.05% bovine serum albumin, 0.15 moles/liter of NaCl). Sections were incubated for 2 hours at 37°C in 25 μl of TdT solution containing 1× terminal transferase buffer, 0.5 nmoles of biotin-labeled dUTP, and 10 units of TdT.

After the TdT reaction, sections were soaked in TdT blocking buffer (300 nmoles/liter of NaCl, 30 mmoles/liter of trisodium citrate-2-hydrate), incubated with horseradish peroxidase (HRP)–conjugated streptavidin for 30 minutes at room temperature, and developed for 10 minutes in phosphate buffered citrate (pH 5.8) containing 0.6 mg/ml of 3,3′-diaminobenzidine tetrahydrochloride dihydrate (DAB). Nuclei were counterstained with methyl green.

Flow cytometric analysis. Surface markers were identified with monoclonal antibodies (mAb) and using an Epics flow cytometer (Beckman Coulter, Miami, FL). Rat mAb against fluorescein isothiocyanate (FITC)–, phycoerythrin (PE)–, or PE-Cy5–conjugated anti-B220, Thy1.2, CD4, and CD8 (eBioscience, San Diego, CA) were used. For detection of T cell activation makers, FITC-conjugated anti-CD25, anti-CD44, anti-CD62L, and anti-CD69 mAb (eBioscience) were used. For detection of B cell surface IgM and IgG1, FITC-conjugated anti-IgM (eBioscience) and anti-IgG1 (BD Phar-

Mingen, San Diego, CA) mAb were used. PE-conjugated anti-Ly5.2 (eBioscience) and biotin-conjugated anti-V_β5.2 and PE-Cy5–conjugated streptavidin (both from BD PharMingen) were used for in vivo ovalbumin-specific T cell expansion. Data were analyzed with FlowJo FACS analysis software (Tree Star, Ashland, OR).

Transfer of OT-2 T cells. Purified CD4+ T cells (5×10^6) derived from the spleen of transgenic OT-2 mice were labeled with carboxyfluorescein succinimidyl ester (CFSE; Molecular Probes, Eugene, OR) and transferred intravenously into B6 (Ly5.1+) mice. One day later, ovalbumin peptide (100 μg) was injected intraperitoneally and rebamipide (0–200 μM; 250 μl per mouse) was injected intravenously into recipient mice. Three days later, cell division was evaluated by flow cytometry to detect the CFSE dilution of the Ly5.2+,V_β5.2+, CD4+ T cells.

Real-time quantitative reverse transcription–polymerase chain reaction analysis. Total RNA was extracted from cultured T cells and B cells derived from the spleen of NFS/*sld* mice with Isogen (Wako Pure Chemical), and reverse transcribed. Transcript levels of NF-κB, FasL, interferon regulatory factor 4 (IRF-4), B lymphocyte–induced maturation protein 1 (BLIMP-1), and β-actin were determined with a PTC-200 DNA Engine Cycler (MJ Research, Waltham, MA) with SYBR Premix Ex Tag (Takara, Kyoto, Japan). The following primer sequences were used: for NF-κB, 5′-ATGGCAGACGATGATCCCTA-3′ (forward) and 5′-TAGGCAAGGTCAGAATGCAC-3′ (reverse); for FasL, 5′-ACTGGACAGATATGGGCCCAC-3′ (forward) and 5′-GCCTCTGTGAGGTAGTAAGTAG-3′ (reverse); for IRF-4, 5′-GAAGCCCCAAAGCCCTCAGTCGTTG-3′ (forward) and 5′-CGCTGAGGAGGAAACTGAA-3′ (reverse); for BLIMP-1, 5′-CATTCCTGTCCCCAACGCATCAACTG-3′ (forward) and 5′-GGTGCCCAAGCACCAAAGTCATAG-3′ (reverse); and for β-actin, 5′-GTGGGCCGCTCTAGGCACCA-3′ (forward) and 5′-CGGTTGGCCTTAGGGTTCAGGGGGG-3′ (reverse). Results were calculated with DNA Engine Opicon System software (Roche Molecular Systems, Alameda, CA).

Western blot analysis. Cell extracts from the nucleus and cytoplasm of T cells and B cells were prepared using a Nuclear/Cytosol Fractionation kit (BioVision, Mountain View, CA). Cells were briefly washed, collected in ice-cold phosphate buffered saline (PBS) in the presence of phosphatase inhibitors, and centrifuged at 500 revolutions per minute for 5 minutes. The pellets were resuspended in a hypotonic buffer, treated with detergent, and centrifuged at 14,000*g* for 30 seconds. The cytoplasmic fraction was collected, the nuclei were lysed, and nuclear proteins were solubilized in lysis buffer containing protease inhibitors. A total of 10 μg of each sample per well was used for sodium dodecyl sulfate–polyacrylamide gel electrophoresis. After blocking with 5% nonfat milk, the membrane was incubated with primary antibodies against phospho-IκBα and NF-κB p65 (RelA) (Santa Cruz Biotechnology, Santa Cruz, CA). Antigen–antibody complexes were detected using a HRP-conjugated secondary antibody. Protein binding was visualized with enhanced chemiluminescence Western blotting reagent (Amersham Biosciences, Arlington Heights, IL). Anti-mouse histone H1 or GAPDH monoclonal antibody (Santa Cruz Biotechnology) was used as the control for protein loading.

Measurement of fluid secretion. Analysis of tear and saliva volumes in rebamipide-treated thymectomized NFS/*sld* mice was performed according to a previously described method (24).

Proliferation assay. CD4+ T cells (1×10^5) purified from spleen cells using anti-B220 mAb, anti-CD8 mAb, and anti-rat IgG conjugated to magnetic beads (Dynal, Oslo, Norway) were placed in RPMI 1640 containing 10% fetal calf serum (FCS), 100 units/ml of penicillin, 0.1 mg/ml of streptomycin, and 50 μM 2-mercaptoethanol and were stimulated with recombinant α-fodrin protein (JS-1) (25) or with plate-coated anti-CD3 and anti-CD28 mAb in 96-well, flat-bottomed plates for 72 hours. Then, ^{3}H-thymidine (1 μCi/well; NEN Life Science Products, Boston, MA) was pulsed into the cell mixture during the final 20 hours of culture. Incorporation of ^{3}H-thymidine was assayed with an automated liquid scintillation counter.

For detection of the proliferation of the CD4+ T cell subset, CFSE-labeled CD4+ T cells were cultured for 72 hours. The CD4+ T cells were then stained with anti-CD4 mAb, and cell division of the CD4+ gated T cells was analyzed by flow cytometer.

Assay of immunoglobulin secretion from B cells. B cells (1×10^5) purified from spleen cells using anti-CD4 mAb, anti-CD8 mAb, and anti-rat IgG conjugated to magnetic beads (Dynal) were placed in RPMI 1640 containing 10% FCS, penicillin/streptomycin, and 2-mercaptoethanol and were stimulated with 10 μg/ml of lipopolysaccharide (LPS; Sigma, St. Louis, MO) and 50 ng/ml of interleukin-4 (IL-4; eBioscience) in 96-well round-bottomed plates for 5 days. Cell surface expression of IgM and IgG1 was detected by flow cytometric analysis, and secreted IgM and IgG1 in the culture supernatants were measured by enzyme-linked immunosorbent assay (ELISA).

Serum autoantibody and cytokine ELISAs. JS-1, SSA/Ro, SSB/La, or single-stranded DNA (ssDNA) antibody was used to coat 96-well plates (24). After the plates were washed, diluted mouse sera were added. HRP-conjugated anti-mouse IgG (heavy and light chains; Vector, Burlingame, CA) was added as the secondary antibody, and *o*-phenylenediamine (OPD; Sigma) buffer was added. Antibodies were measured with an ELISA reader (Model 680; Bio-Rad, Richmond, CA) and with a spectrophotometer at 490 nm.

Serum immunoglobulins were determined by ELISA using a mouse immunoglobulin quantitation kit (Bethyl Laboratories, Montgomery, TX). Briefly, for the IgM and IgA ELISAs, sera were diluted 1:5,000 in PBS, and for the IgG ELISA, sera were diluted 1:25,000 in PBS. Plates were coated with a capture antibody and then washed with PBS–0.1% Tween 20. Diluted sera or culture supernatants were added to the plates and incubated. After washing with PBS–0.1% Tween 20, an HRP-conjugated detection antibody was added. Plates were again washed with PBS–0.1% Tween 20, and OPD buffer was added. Plates were then analyzed with a spectrophotometer at 490 nm, as described previously (26).

Levels of IL-2, interferon-γ (IFNγ), IL-4, and IL-10 in culture supernatants from splenic CD4+ T cells stimulated with anti-CD3 and anti-CD28 for 72 hours were determined by ELISA. Specific antibodies for each cytokine were used in the ELISAs, as previously described (27).

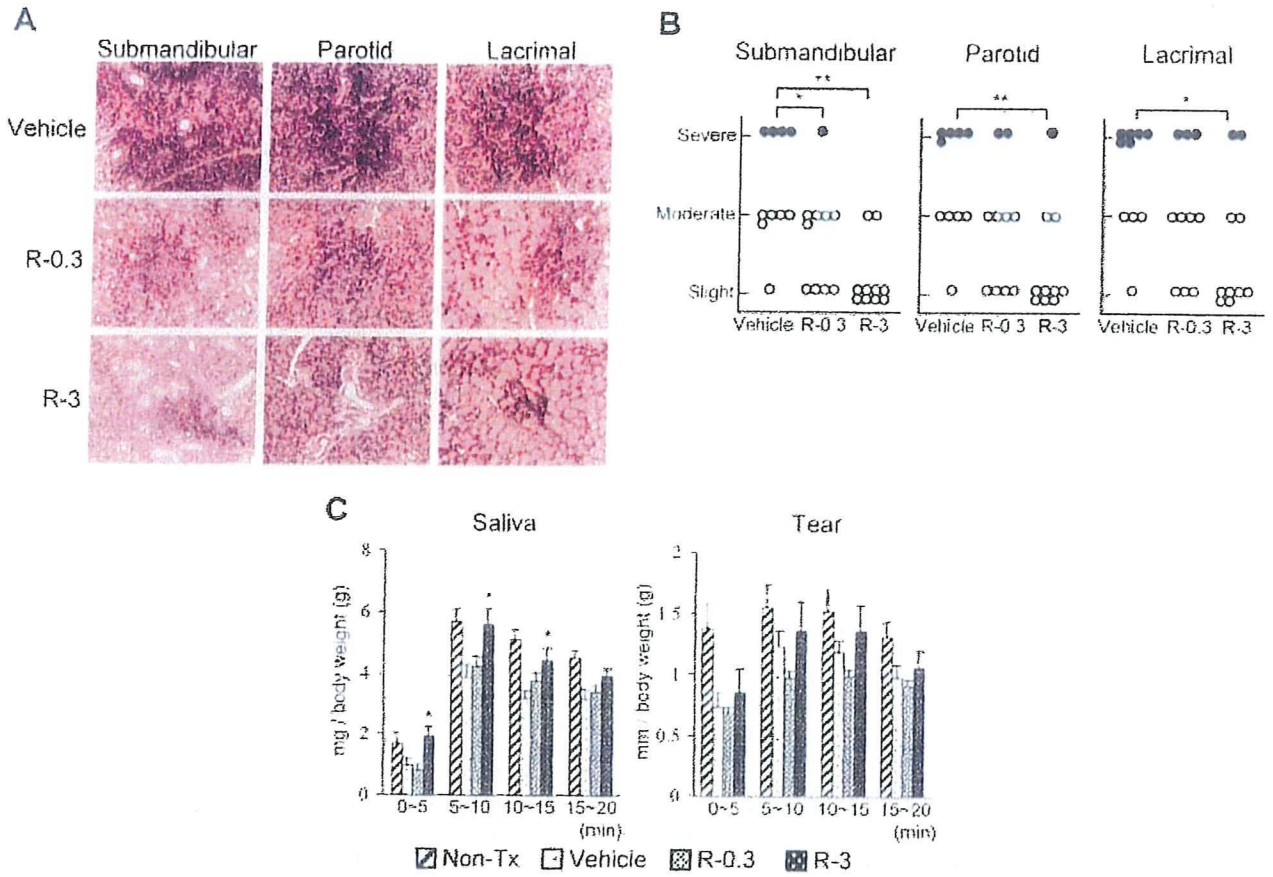

Figure 1. Therapeutic effect of rebamipide on autoimmune lesions in the NFS/*sld* mouse model of Sjögren's syndrome. Mice underwent thymectomy on day 3 after birth and were treated with vehicle, 0.3 mg/kg of rebamipide (R-0.3), or 3 mg/kg of rebamipide (R-3) from age 4 weeks to age 8 weeks. **A,** Sections of salivary and lacrimal glands from the 3 groups of mice. Results are representative of 10 mice per group (hematoxylin and eosin stained; magnification × 100). **B,** Histologic grading of inflammatory lesions in salivary and lacrimal glands from individual mice in the 3 treatment groups. * = $P < 0.05$; ** = $P < 0.01$ by lower-tailed Shirley-Williams test. The mean ± SD histology sores in the vehicle, rebamipide 0.3 mg/kg, and rebamipide 3 mg/kg groups were 2.3 ± 0.7, 1.7 ± 0.7, and 1.2 ± 0.4 for the submandibular glands, 2.4 ± 0.7, 1.8 ± 0.8, and 1.4 ± 0.7 for the parotid glands, and 2.5 ± 0.7, 2.0 ± 0.8, and 1.6 ± 0.8 for the lacrimal glands, respectively. **C,** Average saliva and tear volumes after pilocarpine administration (5 mg/kg) in mice of the 3 treatment groups and in a group of nonthymectomized (non-Tx), vehicle-treated mice at different time periods after pilocarpine administration. Values are the mean and SEM of 10–12 mice per group. * = $P < 0.05$ versus the vehicle-treated control group, by Dunnett's test.

Statistical analysis. Statistical analysis was performed using the Jonckheere trend test and the lower-tailed Shirley-Williams test, Dunnett's test, Student's *t*-test, and chi-square test, as appropriate.

RESULTS

Therapeutic effect of oral administration of rebamipide. In our previous study (22), we found that NFS/*sld* mice subjected to thymectomy on day 3 after birth began to develop autoimmune lesions of the salivary and lacrimal glands at 4 weeks of age or later, while no inflammatory lesions were observed in nonthymectomized NFS/*sld* mice. In the present study, we investigated whether oral administration of rebamipide protects NFS/*sld* mice against the development of autoimmune lesions. To evaluate whether rebamipide treatment was effective at preventing the SS autoimmune pathology, the drug or vehicle alone was administered orally each day to thymectomized NFS/*sld* mice beginning at the age of 4 weeks and continuing to the age of 8 weeks, then organs were removed for histologic analysis.

Salivary and lacrimal glands were stained with hematoxylin and eosin, and histologic features were assessed. Treatment with rebamipide at a concentration of 3 mg/kg prevented the development of autoimmune

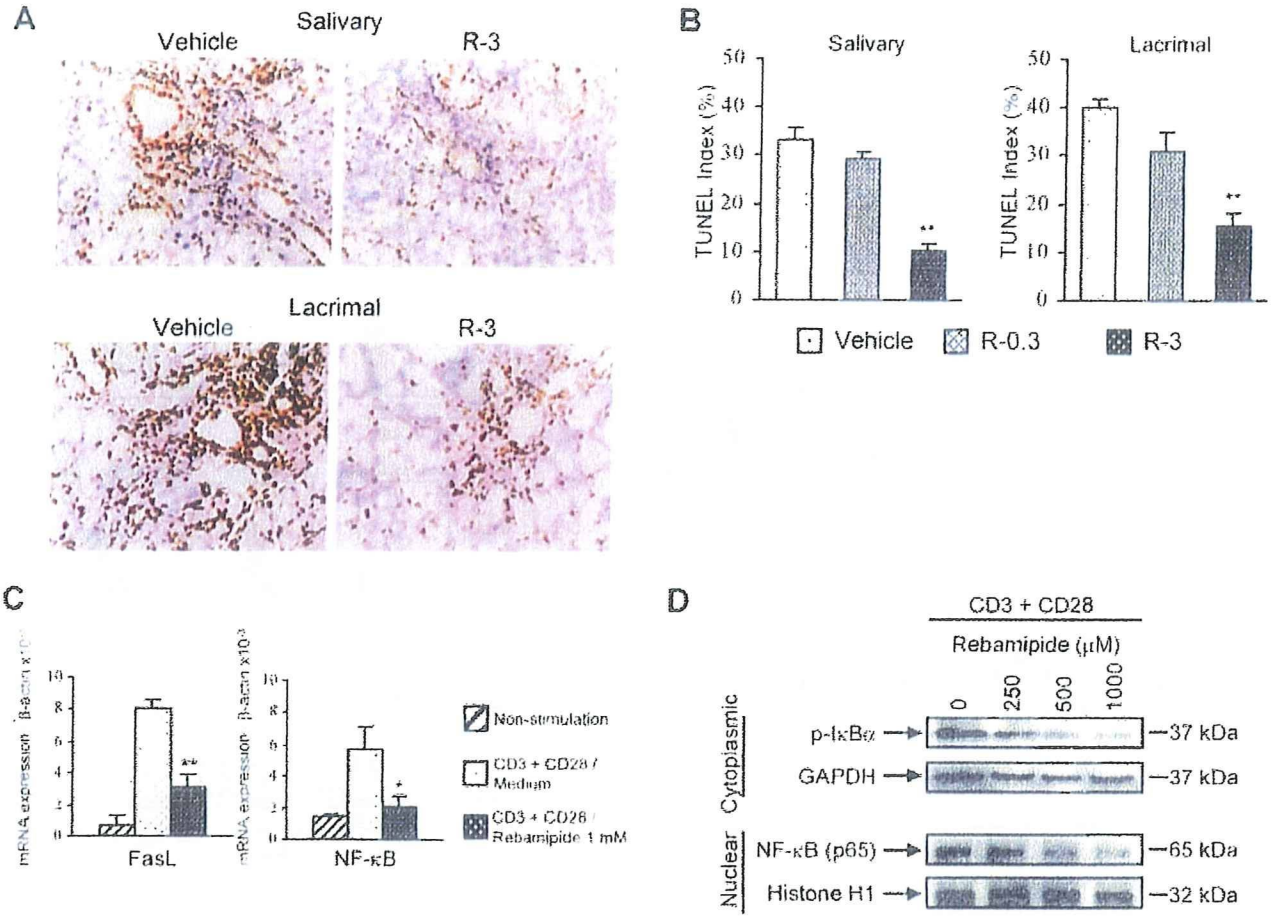

Figure 2. Inhibitory effect of rebamipide on apoptosis of salivary gland cells in the NFS/*sld* mouse model of Sjögren's syndrome. Mice underwent thymectomy on day 3 after birth and were treated with vehicle, 0.3 mg/kg of rebamipide (R-0.3), or 3 mg/kg of rebamipide (R-3) from age 4 weeks to age 8 weeks. **A,** TUNEL assay for apoptotic cells in the salivary and lacrimal glands of mice treated with vehicle or with 3 mg/kg of rebamipide. Results are representative of 5–8 mice per group (magnification × 100). **B,** Percentages of TUNEL+ salivary and lacrimal epithelial cells in the 3 treatment groups. Positive cells were enumerated using a 10 × 20–μm grid net disc covering an objective area of 0.16 mm^2 (n = 10 fields per section). Values are the mean and SEM of 5 mice per group. ** = $P < 0.01$ versus the vehicle-treated group, by Dunnett's test. **C,** Inhibitory effect of rebamipide on T cell activation. Purified CD4+ T cells derived from mouse spleens were stimulated with plate-coated anti-CD3 and anti-CD28 monoclonal antibody for 2 hours in the presence of rebamipide. Levels of mRNA for FasL and NF-κB were detected by quantitative reverse transcription–polymerase chain reaction analysis. Values are the mean and SEM expression relative to β-actin mRNA in triplicate wells. * = $P < 0.01$; ** = $P < 0.05$ versus medium containing anti-CD3 and anti-CD28, by Student's *t*-test. **D,** Phosphorylation of IκB and nuclear translocation of NF-κB in cytoplasmic and nuclear extracts of activated CD4+ T cells treated with CD3 and CD28 ligation in the presence of rebamipide, as analyzed by Western blotting. GAPDH and histone H1 were used as the respective internal controls. Results are representative of 3 independent experiments.

lesions in the submandibular ($P < 0.01$), parotid ($P < 0.01$), and lacrimal ($P < 0.05$) glands (Figures 1A and B). Rebamipide treatment at a concentration of 0.3 mg/kg prevented the development of autoimmune lesions in the submandibular glands alone ($P < 0.05$). Mononuclear cell infiltration as well as destruction of the parenchyma was inhibited in the salivary and lacrimal glands of thymectomized NFS/*sld* mice treated with rebamipide. The average saliva volume, but not tear volume, in the rebamipide-treated group was significantly higher than that in the vehicle-treated control group (Figure 1C).

We previously demonstrated that epithelial cell apoptosis via the Fas/FasL system plays an important role in the development of autoimmune lesions in this mouse model of SS, and a significant increase in TUNEL+ apoptotic epithelial duct cells in the salivary glands was detected in this mouse model (11). In the